A STRUCTURAL AND VAPORIZATION
EXAMINATION OF YTTERBIUM(II)
CHLORIDE AND YTTERBIUM(III)
OXIDECHLORIDE

Thesis for the Degree of Ph. D.
MICHIGAN STATE UNIVERSITY
NORMAN ALLEN FISHEL
1970



This is to certify that the

thesis entitled

A STRUCTURAL AND VAPORIZATION EXAMINATION

OF YTTERBIUM(II) CHLORIDE AND YTTERBIUM(III) OXIDECHLORIDE

presented by

Norman Allen Fishel

has been accepted towards fulfillment of the requirements for

Ph.D. degree in Chemistry

Dr. H.A. Eick

Major professor

Date May 15, 1970



ABSTRACT

A STRUCTURAL AND VAPORIZATION EXAMINATION OF YTTERBIUM(II) CHLORIDE AND YTTERBIUM(III) OXIDECHLORIDE

bу

Norman Allen Fishel

The crystal structure of ytterbium(II) chloride has been determined from an X-ray diffraction study of a single crystal specimen. Eight formula units are contained in an orthorhombic cell (a = 6.693±0.001, b = 13.149±0.003, and c = 6.943±0.001 Å); space group P 2₁/b 2₁/c 2₁/a. The final R factor is 0.137 for three-dimension counter data collected with CuKa radiation. YbCl₂ crystallizes in the CeSI-type structure. X-Ray powder diffraction data for ytterbium(III) oxidechloride have been indexed on a hexagonal cell (a = 3.726±0.002 and c = 55.61±0.08 Å), the dimensions of which were obtained from single crystal diffraction data. TmOC1, LuOC1, and mixed lanthanide oxidechlorides whose average cationic radius is smaller than the Er(III) radius are isostructural with YbOC1. An intermediate chloride, YbCl_{2.26}, has been prepared.

The vaporization reaction (1) of YbCl₂ was characterized by a YbCl₂(ℓ) = YbCl₂(g) (1)

combination of X-ray diffraction, weight loss, effusate collection, and high temperature mass spectrometric techniques. Equilibrium vapor pressure measurements (1048 ≤ T ≤ 1483°K) for reaction (1) have been made by target collection-Knudsen effusion technique. At the median temperature, 1265 °K, the second law enthalpy and entropy of

Norman Allen Fishel

vaporization were: ΔH_{V}° 1265 = 55.2±1.1 kcal mole⁻¹ and ΔS_{V}° 1265 = 21.3±0.9 eu. At the extrapolated boiling point (2242 °K), YbCl₂(£) has a second law enthalpy and entropy of vaporization of: ΔH_{V}° 2242 = 46.8±3.5 kcal mole⁻¹ and ΔS_{V}° 2242 = 20.8±1.5 eu. At 298 °K the following values were obtained: YbCl₂(s)— ΔH_{V}° 298 (2nd Law) = 61.2±2.3 kcal mole⁻¹, ΔS_{V}° 298 = 31.1±2.0 eu, and ΔH_{V}° 298(3rd Law) = 59.7±0.8 kcal mole⁻¹. The enthalpy and free energy of formation and the standard entropy calculated from second law results are: YbCl₂(s) - ΔH_{f}° 298 = -181.8±3.6 kcal mole⁻¹, ΔG_{f}° 298 = -175.3±3.6 kcal mole⁻¹, and S_{298}° = 30.7±2.5 eu. Reaction (2) is proposed as the decomposition 3YbOCl(s) = Yb₂O₃(s) + YbCl₂(s) + Cl(g) (2)

mode for YbOC1 and thermodynamic data have been estimated for the reaction.

A STRUCTURAL AND VAPORIZATION EXAMINATION OF YTTERBIUM(II) CHLORIDE AND YTTERBIUM(III) OXIDECHLORIDE

Ву

Norman Allen Fishel

A THESIS

Submitted to

Michigan State University

in partial fulfillment of the requirements

for the degree of

DOCTOR OF PHILOSOPHY

Department of Chemistry

1970

G-65414

ACKNOWLEDGEMENTS

The author is especially indebted to Professor Harry A. Eick for his guidance and personal interest throughout the course of this research.

This work would not have been possible without the encouragement, support, and patience of my wife Grace. The author is particularly grateful for her understanding.

Particular thanks are due to my colleagues in the High Temperature Group. Their concern and suggestions and the rapport of the laboratory were very helpful in producing these results. The help extended by the departmental shops was invaluable in establishing some of the experimental apparatus.

Financial support of this research by the United States Atomic Energy Commission under contract number AT (11-1)-716 has been very welcome.

TABLE OF CONTENTS

			Page
I.	Int	roduction	1
II.	Previous Investigations of the Ytterbium-Oxygen-Chlorine System		
	Α.	Ytterbium Chlorides 1. Preparative and Structural Investigations 2. Thermochemical Investigations	3 3 5
	В.	Ytterbium Oxidechloride 1. Preparative and Structural Investigations 2. Thermochemical Investigations	7 7 7
	c.	Other Ytterbium Halides and Oxidehalides 1. Fluorides 2. Bromides 3. Iodides 4. Astatides	8 8 8 8
	D.	Relevant Non-ytterbium Chlorides and Oxidechlorides	8
III.	The	oretical Considerations Applicable to This Investigation	12
	Α.	 Thermodynamic Phase Relationships and Vaporization Behavior Vapor Pressure Measurements Knudsen Effusion Requirements and Assumptions Target Collection Analysis of the Collected Effusate Temperature Measurement Identification of Vapor Species Thermodynamic Calculations Second Law Method Third Law Method Sources of Thermodynamic Data 	12 13 13 13 15 16 17 18 18 18 20 21
	В.	Structural Determination 1. Unit Cell Determination a. Optical Properties b. Symmetry Elements and Systematic Absences c. Unit Cell Axial Lengths and Space Group d. Density Measurements 2. Intensity Data Collection a. Eulerian Geometry Diffractometer b. Eulerian Axes	21 22 23 23 24 24 26
		 c. Crystal Monochromator d. Intensity Data Collection Techniques 	27 29

TABLE	OF	CONTENTS	(Cont.)	Page
		3. Data	a Reduction	31
		a.	Geometrical Factors	31
			(1) Polarization Factor	31
			(2) Lorentz Factor	31
			(3) Monochromator Factor	32
		ъ.	Physical Factors	32
			(1) Absorption	32
			(2) Extinction	33
		4. Sol	ution of the Structure	33
		a.	Fourier Synthesis	34
		ъ.	Patterson Synthesis	34
		c.	Least Squares Refinement	35
			(1) Thermal Parameters	35
			(2) Anomalous Dispersion	36
IV.	Exp	perimenta	1 Materials, Equipment, and Procedures	37
	Α.	Materia	ls	37
	В.	Sample 1	Preparation	37
			erbium Trichloride Hexahydrate	37
			erbium Trichloride	37
		a.	Thionyl Chloride	38
		b.	Chloroform	38
		c.		38
			Chlorine	38
			Hydrogen Chloride	39
		f.	Ammonium Chloride	39
			erbium Dichloride	39
		a.	Metallothermic Reduction	39
		b.	Thermal and Hydrothermic Reduction	40
			erbium Oxidechloride	40
			er Oxidechlorides	40
		a.	Triytterbium Tetraoxidechloride	40
		b.		40
	C.	Single	Crystal Growth	41
	D.		cal Techniques	41
			orine Analysis	41
			erbium Analysis	41
		3. 0xy	gen Analysis	42
	E.	Density	Measurement	42
	F.		echniques	42
		1. Pow	der Methods	42
		2. Sin	gle Crystal Methods	43
		a.	Optical Examination	43
		ъ.	Cameras	44

TABLE	OF	CONTENTS	(cont.)	Page
		c.	Eulerian Cradle	44
		d.	Monochromator	44
		e.	Crystal Orientation	44
		f.	Lattice Parameter Refinement	45
		g.	Intensity Data Collection	45
		3. Flu	orescence Methods	46
		a.	Spectrometer Operation	46
		ъ.	Spectrometer Calibration	46
	G.	Neutron	Activation Analysis	47
	н.		ation Mode Characterization	47
			ght Loss Measurements	47
			s Spectrometric Investigation	47
			usate Collection	48
		4. X-ra	ay Examination	48
	I.		Collection Technique	48
			eral Procedure	48
			perature Measurement fice Measurement	48
				48
			usion Cell Design densation Coefficient Determination	49
		J. Cond	lensation Coefficient Determination	49
	J.	Auxilary	y Equipment	51
v.	Res	sults		52
	A. Preparative		52	
			erbium Trichloride Hexahydrate	52
			erbium Trichloride	52
			ermediate Ytterbium Chloride (YbCl _{2.26})	54
			erbium Dichloride	54
			erbium Oxidechloride	55
		6. Oth	er Oxidechlorides	56
	В.	Structural		
			t-Cell Determination	57
		a.	Optical Properties	57
		ъ.	Systematic Absences and Space Group Lattice Parameters	57 50
		c. d.		58 50
			Density	58
		2. III.	ensity Data Data Collection	60 60
		а. b.	Absorption Correction	60
			putations	61
			terson Synthesis and Ytterbium Atom Positions	61
			ution of the Chlorine Atom Positions	63
	C. Thermodynamic			
	- •	7	ay Fluorescence Calibration	66 66
			tron Activation Analysis	66
			densation Coefficient	66

TABLE	OF	CONTENTS (cont.)	Page			
		4. Temperature Measurement	66			
		5. Orifice Closure	67			
		6. Vaporization Mode	67			
		a. Weight Loss	67			
		b. Mass Spectrometer	67			
		c. Effusate Collection	68			
		d. X-Ray Examination	68			
		7. Vapor Pressure Equation	68			
		8. Thermodynamic Values Employed in Data Reduction	68			
		9. Thermochemical Values	71			
VI.	Discussion					
	A.	Evaluation of Experimental Conditions	73			
		1. Neutron Activation Analysis	73			
		2. Fluorescence Analysis	73			
		3. Temperature Measurements	74			
		4. Orifice Closure	74			
		5. Knudsen Conditions	75			
		6. Crucible Materials	75			
		7. Density Measurement	75			
		8. Intensity Data Collection	75			
	В.	Evaluation of Thermochemical Values Obtained	76			
		1. Vaporization Mode	76			
		2. Thermodynamic Approximations	76			
		3. Ytterbium Dichloride Data	77			
	c.	Structure of Ytterbium Dichloride	78			
	D. Structure of Ytterbium Oxidechloride					
	E.	Decomposition of Ytterbium Oxidechloride	85			
	F.	On Ytterbium(II) as a Group IIB Ion	86			
VII.	Suggestions for Future Research					
	REI	FERENCES	89			
	API	PENDICES	97			

LIST OF APPENDICES

APPEND	IX	Page	
ı.	Properties of Ytterbium Halides		
II.	Orientation and Angle Setting Program	98	
III.	X-Ray Powder Diffraction Data		
	A. Ytterbium Trichloride Hexahydrate B. Intermediate Ytterbium Chloride (YbCl _{2.26}) C. Ytterbium Dichloride D. Ytterbium Oxidechloride E. Triytterbium Tetraoxidechloride Preparation	100 101 101 102 102	
IV.	Equilibrium Pressure and Third-Law Enthalpy Data	103	
v.	Thermodynamic Values for Data Reduction	105	

LIST OF TABLES

TABLE		Page
ı.	Analytical Results	53
II.	Lattice Parameters	53
III.	Properties of Space Group Pbca	59
IV.	Positions and Heights of Principal Patterson Peaks	62
v.	Parameters from Least-Squares Refinement A. Atomic Coordinates B. Thermal Parameters	64
VI.	Observed and Calculated Structure Factors	65
VII.	Experimental Thermochemical Data	80
VIII.	Compounds with the CeSI-type Structure	80

LIST OF FIGURES

FIGURE		Page
1.	A Four-circle Normal Beam Eulerian Cradle	25
2.	Eulerian Axes	28
3.	Diffractometer and Monochromator Optics	30
4.	Effusion Cell Enclosed in Graphite Oven	50
5.	Representation of Space Group Pbca	59
6.	Appearance Potential Curves	69
7.	Pressure of YbCl ₂ (g) in Equilibrium with YbCl ₂ (l)	70
8.	Atomic Packing in YbCl ₂	79
9.	Chlorine Environment in YbCl ₂	81

CHAPTER I

INTRODUCTION

The pedagogical practice of placing strong emphasis upon various trends and groupings within the periodic table has resulted in neglect of the individuality of the various lanthanides. Although many chemists today are aware that the term "rare earth" is a misnomer, few are aware of the fact that anomalies of chemical behavior are common place among the lanthanides. Industrial interest in the chemistry of the lanthanides has increased greatly with the advent of lanthanide-doped yttrium garnets for lasers, samarium-cobalt alloys for permanent magnets, mixed metal lanthanide petroleum catalysts, and europium phosphors for color television tubes. Prior uses for the lanthanides were limited to glass decolorization for example and nuclear reactor technology in which the lanthanides are fission by-products.

The chemistry of ytterbium has been neglected frequently in general lanthanide studies. While no count has been made, it is the author's opinion that the number of literature citations of ytterbium chemistry exceeds only those of promethium which does not occur naturally, and lutetium, the least abundant of the "rare earths." Inattention to ytterbium chemistry no doubt is in part due to the stability of both di- and trivalent ytterbium. Although trivalent ytterbium chemistry largely parallels the chemistry of the other heavy lanthanides, divalent ytterbium chemistry often contrasts with both the other divalent

lanthanides and with the alkaline earths which have been used as models.

The existence of mixed di- and trivalent chemistry introduces yet another complexity to the study of ytterbium compounds.

The nature of lanthanide group VIA and VIIA compounds is such that they often lend themselves to high temperature applications. Lack of knowledge about simple binary and ternary compounds in part limits application of the lanthanides to new uses. To make possible design of materials for use at elevated temperatures, it is frequently necessary to understand the nature of the chemical bonding. Two techniques, vaporization and crystal structure determination, were used in this investigation to aid in the comprehension of the bonding in the ytterbium-oxygen-chlorine system. The work for the most part was restricted to an examination of ytterbium(II) chloride and ytterbium(III) oxidechloride with ancillary examination of related phases.

CHAPTER II

PREVIOUS INVESTIGATIONS OF THE YTTERBIUM-OXYGEN-CHLORINE SYSTEM

The halides, halo-complexes and oxidehalides of the lanthanide and actinide elements together with those of scandium and yttrium have been reviewed thoroughly in the recent book by Brown. The literature through 1967 was examined extensively and the book is recommended as a concise compilation of the then available information on preparation, structure, and thermochemistry.

A. Ytterbium Chlorides

1. Preparative and Structural Investigations

The first significant work on the ytterbium chlorides was carried out by Klemm, Jantsch and their co-workers 2-8. Their work was greatly encumbered by the unavailability of pure lanthanide oxides. The ytterbium sesquioxide used by Klemm and Schüth³ for preparation of ytterbium dichloride contained almost ten percent of other lanthanides as impurities. However reduction of trivalent ytterbia to divalent YbCl₂ was in effect a purification which removed most of the trivalent impurities which are reduced less readily than is ytterbium(III). The X-ray diffraction pattern for YbCl₂ was reported by Döll and Klemm⁷ and was indexed as a pseudo-cubic distorted fluorite structure. Notable work on ytterbium(III) chloride was not undertaken until higher purity ytterbia became readily

available around 1955.

Various methods for preparation of anhydrous lanthanide halides were reviewed by Taylor⁹ and more recently by Johnson and Mackenzie¹⁰. Novikov and Polyachenok¹¹ considered techniques particularly applicable to the preparation of lower valent lanthanide halides. The novel method of preparing in liquid ammonia divalent europium and ytterbium halides free of the corresponding trivalent metal ions was given by Howell and Pytlewski¹², while Mroczkowski¹³ described the preparation of EuCl₃ free of divalent contamination. Anhydrous YbCl₃ crystallizes with the monoclinic aluminum chloride-type structure¹⁴, space group C2/m, which is a distorted sodium chloride structure in which two-thirds of the metal atoms are omitted.

Aqueous solutions of YbCl₃ are prepared readily by dissolution of Yb₂O₃ in concentrated hydrochloric acid. The YbCl₃ which separates from solution is reported to retain six¹⁵⁻¹⁷ to seven¹⁸ waters of crystall-ization. Crystallographic data have been reported for Nd, Sm, and Er¹⁹; Gd²⁰; Eu²¹; Sm, Eu, Gd, Tb, Dy, Ho, Er, and Tm²² hydrated lanthanide trichlorides and all have been identified as isostructural hexahydrates. The structure²⁰ is monoclinic, space group P2/n, and two molecules are in the unit cell. The structure contains complexes of the type [Cl₂Gd(OH₂)₆]⁺ which are held together by O-H··· Cl hydrogen bonds. A third of the chlorine atoms form no bonds with the gadolinium atoms. The shortest bond distance for these atoms is greater than 5 Å which is nearly twice the 2.768 Å Gd-Cl distance for the other chlorine atoms. Heptahydrated YbCl₃ is reported¹⁸ to undergo thermal decomposition to tetra- di-, and monohydrates before anhydrous YbCl₃ is formed. There are no reports of hydrates of YbCl₂. Ammoniated YbCl₁ is reported¹² to

lose ammonia of crystallization upon slight heating or to undergo decomposition³ to an amidechloride according to equation (II-1).

$$YbC1_2 \cdot xNH_3(s) = Yb \cdot NH_2 \cdot C1_2(x-1)NH_3(s) + 1/2H_2(g)$$
 (II-1)

Johnson and Mackenzie¹⁰ attempted direct conversion of samarium and ytterbium metals to the dichlorides by an adaptation of Druding and Corbett's²³ method for preparation of the trichlorides. The metals were heated at 900° under a H₂-HCl mixture and then cooled under hydrogen alone. The dull green ytterbium product was completely water soluble and elemental analyses were consistent with a composition of 3YbCl₃·5YbCl₂. The samarium product was in the form of lustrous black crystals which exhibited a 0.9% chlorine deficiency (presumed by this author to be with respect to the dichloride composition). The X-ray diffraction data were reported in Mackenzie's Ph.D. Thesis, University of London, 1968, and are not available in the open literature. Efforts by Polyachenok and Novikov²⁴ to obtain SmCl₂ by reduction of SmCl₃ with zinc metal always yielded a product containing unreduced SmCl₃ with a composition of SmCl₃·4SmCl₂.

2. Thermochemical Investigations

Only limited experimental thermochemical data have been reported for the lanthanide halides. These data are reported in part in Table VII in Chapter VI. The enthalpies of formation of all lanthanide trichlorides other than promethium, ytterbium, and lutetium were determined by Bommer and Hohman²⁵. Their values (which are listed in NBS Circular 500²⁶) have been shown²⁷⁻²⁹ to be up to 10 kcal mole⁻¹ too high. Brewer et al.^{30,31} estimated thermochemical values for both ytterbium trichloride and dichloride.

Polyachenok and Novikov³² estimated the enthalpies of formation of all the lanthanide dichlorides by using Born-Haber cycles. On the basis of their estimates, they concluded that all lanthanide monochlorides are unstable in the condensed state with respect to disproportionation. By the boiling point method^{33,34} the saturated vapor pressures of SmCl₂, EuCl₂, and YbCl₂ were measured. From these data it was concluded that these dichlorides vaporize without decomposition. Conversely, NdCl₂ was not observed in the sublimate even though its presence in the Nd-NdCl₃ system has been confirmed²³. The enthalpy of formation of YbCl₂ has also been determined calorimetrically³⁵⁻³⁷ by dissolution in 6M HCl. Recently Johnson³⁸ has recalculated the enthalpies of formation of the lanthanide dichlorides by employing more recent thermodynamic data.

Spedding and Flynn^{28,29} have shown a monotonic relationship between the enthalpies of formation of the lanthanide trichlorides obtained from the enthalpies of solution of the anhydrous chlorides and the atomic number of the metal. Results of the two vaporization studies of YbCl₃ are not in agreement. Moriarity³⁹ using Knudsen effusion found YbCl₃ to vaporize congruently without decomposition to YbCl₂, while Polyachenok and Novikov⁴⁰ measured the decomposition pressures of SmCl₃, EuCl₃, and YbCl₃ according to reaction (II-2). The enthalpies of formation of YbCl₃ and

 $LnCl_3(l) = LnCl_2(l) + 1/2Cl_2(g)$ Ln = Sm, Eu, Yb (II-2) $TmCl_3$ were measured by Stuve⁴¹ using solution calorimetry. By considering the reactions of the various lanthanide halides with the respective metals, Novikov and $Baev^{42}$ have determined the free energies of dissociation of YbCl₃ and YbCl₂.

Ashcroft and Mortimer¹⁸ have reported the thermal decomposition profiles and enthalpies of decomposition of the lanthanide(III) chloride

hydrates. The DTA curve for YbCl₃·7.4H₂O shows four maxima in the rate of enthalpy change versus temperature.

B. <u>Ytterbium Oxidechloride</u>

1. Preparation and Structural Investigations

The oxidechlorides of the type LnOCl have been prepared for all lanthanides except promethium by Templeton and Dauben⁴³ by heating sesquioxide in a mixture of hydrogen chloride and water vapor. Several oxidechlorides, including YbOCl, have been prepared^{44,45} by thermally decomposing the hydrated perchlorates.

Wendlandt^{15,16} studied the thermal decomposition of YbCl₃·6H₂O and observed four inflection points in the thermogram. Although the composition at the first point (145°) was not determined, the second point corresponded to a formula of YbOCl·2YbCl₃. Further weight loss took place until at 395° the composition was YbOCl. Decomposition to the oxide began at 585°. Haesler and Matthes¹⁷ have investigated the thermal dehydration of a YbCl₃·6H₂O sample confined under a mixture of air and hydrogen chloride. They reported as successive dehydration products YbCl₃·3.5H₂O, YbCl₃·2H₂O, YbCl₃·H₂O, YbCl₃, and YbOCl, but not the temperatures at which these changes took place.

Templeton and Dauben⁴³ stated that the oxidechlorides of thulium, ytterbium, and lutetium have an undetermined structure different from the PbFC1-type structure exhibited by the other lanthanide oxidechlorides. They found ErOC1 to exist in both structural types.

2. Thermochemical Investigations

Morozov and Korshunov^{46,47} indicated that both the chlorination of the sesquioxide and the displacement of chlorine by oxygen according to equation (II-3) occurs in one stage without formation of any intermediate

 $2 \text{Ln}_2 \text{O}_3(\text{s}) + 6 \text{Cl}_2(\text{g}) = 4 \text{Ln} \text{Cl}_3(\text{s}) + 3 \text{O}_2(\text{g})$ Ln = La, Nd (II-3) oxidechlorides. Baev and Novikov⁴⁸ studied the disproporationation reaction (II-4) for lanthanum and neodymium and calculated thermochemical $3 \text{LnOCl}(\text{s}) = \text{LnCl}_3(\text{s}) + \text{Ln}_2 \text{O}_3(\text{s})$ Ln = La, Nd (II-4)

values for other lanthanides.

C. Other Ytterbium Halides and Oxidehalides

1. Fluorides

Ytterbium trifluoride is prepared conveniently⁴⁹ by reaction of the sesquioxide with ammonium bifluoride. The compound has been well-characterized and a number of the properties of YbF₃ along with those of other ytterbium halides are given in Appendix I. The vapor species observed^{50,51} during the sublimation of YbF₃ indicated no decomposition to YbF₂. Asprey et al.⁵² had difficulty in obtaining stoichiometric YbF₂ as evidenced by magnetic susceptibility measurements. Bedford and Catalano⁵³ observed a number of phases between the YbF₂ and YbF₃ stoichiometric compositions.

Vorres and Riviello⁵⁴ prepared a series of isomorphous rhombohedral stoichiometric LnOF phases for Y, Dy, Er, Tm, Yb, and Lu by hydrolysis of the respective fluorides at 500°. Podberezskaya et al.⁵⁵ found that hydrolysis of YbF₃ at 600° produced only a mixture of YbOF and Yb₂O₃, but they were able to prepare the rhombohedral YbOF by heating at 800° an equimolar mixture of Yb₂O₃ and YbF₃ confined in a platinum crucible which was sealed in quartz. Shinn⁴⁹ attempted preparation of YbOF but did not report his results. Roether⁵⁶ was unable to confirm the findings of Podberezskaya et al.⁵⁵ but instead found YbOF to crystallize with the

monoclinic lattice of the ZrO₂-baddelite type. There are no reports of non-stoichiometric ytterbium oxidefluorides of the type which have been found for a number of other lanthanides.

2. Bromides

Ytterbium tribromide hexahydrate decomposes⁵⁷ upon heating in air to form a tribromide-oxidebromide mixture which undergoes further oxidation to YbOBr and finally to Yb₂O₃. Anhydrous YbBr₃ decomposes⁵⁸ to YbBr₂ before melting. A more convenient method of preparation of the dibromide is hydrogen reduction of the tribromide. Döll and Klemm⁷ reported YbBr₂ to be isostructural with CaBr₂. A recent single crystal X-ray structure determination of YbBr₂⁵⁹ has refined the earlier⁷ powder diffraction analysis. All of the lanthanides form⁶⁰⁻⁶³ LnOBr oxidebromides with a PbFCl-type structure. Neodymium, samarium, europium, and ytterbium form Ln₃O₄Br-type oxidebromides which possess orthorhombic symmetry^{64,65}.

3. Iodides

The compounds $YbI_3^{66,67}$, $YbI_2^{58,68}$, and $Yb0I^{69-71}$ have been prepared and studied crystallographically. The triiodide is similar to the tribromide in that it decomposes before melting to the lower valent YbI_2 . There are no reports of hydrated iodides or other oxide iodides.

4. Astatides

The ytterbium-astatine system has not been examined.

D. Relevant Non-ytterbium Chlorides and Oxidechlorides

The study conducted by Hastie et al. 72 for LaCl $_3$, EuCl $_3$, EuCl $_2$, and LuCl $_3$ is the only mass spectrometric examination of the lanthanide chlorides. There is evidence of dimerization, perhaps of the Al $_2$ Cl $_6$ type,

for LaCl₃ and LuCl₃ for which enthalpies of dimerization have been measured. No dimerization or significant disproportionation of EuCl₂(g) was found. The sublimation pressures for EuCl₃ were too low to permit useful ion intensity measurements. At temperatures around the melting point of EuCl₃, it decomposed to form EuCl₂⁴⁰.

Natansohn⁷³ has described formation of Y_3O_4C1 analogous to, but not isostructural with, the lanthanide tetraoxidemonobromides^{64,65}. Attempts to synthesize La₃O₄C1 and Gd₃O₄C1 were unsuccessful. Haschke⁷⁴ has found recently that Eu₃O₄Br exhibits at least two polymorphs.

Markovskii et al. 75 studied the thermal decomposition of YOC1·6H₂O and observed compositions of 2YCl₃·YOCl, YCl₃·YOCl, and YCl₃·2YOCl. A compound 2YOCl·Y₂O₃ was isolated and X-ray powder diffraction data were listed. A similar profusion of compounds in a divalent oxide-halide system was reported by Frit et al. 76 for SrX₂-SrO (X = Cl, Br, I).

Haschke⁷⁷ has pointed out that in the ternary system, MOX, where M is a metal with possible divalent and trivalent character and X is a halogen, the general formulation for all stoichiometric phases can be expressed by (II-5). The coefficients ℓ , m, and n may assume integral

 $M_{\ell}O[(3\ell-m)/2] - [n/2]^{X_n}$ (II-5) values in accordance with the restrictions that $\ell \geq 1$, $0 \leq m \leq \ell$, and $0 \leq n \leq (3\ell-m)$. For the lanthanide-oxygen-chlorine system only three of these potential phases have been reported: LnCl₂, LnCl₃, and LnOCl.

There are accounts of lanthanide-oxygen-halogen phases in which the halogen is coordinated to the oxygen rather than the metal but they will not be considered in this work.

During recent years there has been much interest in the $Ln-LnCl_3$ systems. Of particular significance are the studies involving $dysprosium^{78}$ and $thulium^{79}$. In each system a dichloride isostructural with $YbCl_2$ was found.

CHAPTER III

THEORETICAL CONSIDERATIONS APPLICABLE TO THIS INVESTIGATION

A. Thermodynamic

1. Phase Relationships and Vaporization Behavior

Gibbs⁸⁰ in considering the equilibrium of a system stated that it possesses only three independently variable factors - temperature, pressure, and the concentration of the components of the system.

From this he deduced what is now generally known as the Phase Rule (III-1) by which the conditions of equilibrium, F, are defined as

$$F = C - P + 2 \tag{III-1}$$

a relationship between the number of phases, P, and the number of components, C, of the system.

Generally one works with a univariant system, F = 1, such that fixing the temperature fixes the pressure. In a congruent vaporization the composition of the vapor phase is always the same as that of the condensed phase. For a congruent process, P = 2 (the condensed and vapor phases), and F must equal C. For a binary system C = 2, thus F = 2. However, the congruency requirement of constancy of composition provides the additional restriction such that F = 1 and the system is univariant. In other words, the Phase Rule for a congruently vaporizing system is given by equation (III-2).

$$F = C - P + 1 \tag{III-2}$$

2. Vapor Pressure Measurements

There are several ways of measuring vapor pressures of substances. The most common ones are the static, boiling point, transpiration, Knudsen effusion, and Langmuir free-evaporation methods. Each of these techniques is considered in reviews by $Gilles^{81}$ and $Cater^{82}$. The Knudsen effusion method which is suitable for measuring vapor pressures in the range from 10^{-9} to 10^{-3} atmospheres was chosen for this work. From vapor pressure measurements various thermodynamic quantities such as enthalpies, entropies, and free energies of formation may be determined.

3. Knudsen Effusion

a. Requirements and Assumptions

In the Knudsen effusion method a sample is confined in an inert container (called a Knudsen or effusion cell) which can be heated in vacuum. The rate at which a vapor species effuses through a small orifice is then determined. The method is based upon the kinetic theory of dilute gases which requires that the distribution of molecular velocities in a gas at low pressure obeys the Maxwell-Boltzmann law. The term molecule in this usage refers to the gaseous species and does not necessarily imply any regular aggregation of atoms.

The theoretical treatment of effusion was first considered by $Knudsen^{83,84}$ and more recently by $Cater^{82}$. The rate of collision of molecules on unit area of the container wall, Z, in unit time, is given by (III-3) where N/V is the number of molecules per unit volume and \bar{c} is

$$Z = 0.25 \text{Ne/V} \tag{III-3}$$

the average molecular velocity obtained from the kinetic theory (III-4),

$$\bar{c} = (8RT/\pi M)^{1/2} \tag{III-4}$$

with R being the ideal gas constant, M the molecular weight of the

species, and T the absolute temperature. The rate of effusion of molecules into a perfect vacuum per unit time through a small ideal orifice of area A is ZA.

The angular distribution of these effusing molecules is not equally probable in all directions. The randomness of approach leads to the probability (III-5) that a molecule approaches the wall at an angle $\boldsymbol{\theta}$

 $(N(\theta)/Z) = (N/V) \bar{c} \cos \theta (d\omega/4\pi)$ (III-5)

to the normal within the element of solid angle d ω where d ω = 2π sin θ d θ . This result is called the cosine law and it is generally assumed that the effusing molecules obey this law as do those molecules reflected from the wall⁸².

Non-cosine law reflection of real molecules from the walls and orifice yields effusion rates which differ from theoretical values. Wang and Wahlbeck^{85,86} have studied the velocity and angular distributions of the effusate for various orifices. Ward⁸⁷ has examined the validity of the cosine law distribution for conical orifices and has found deviations from ideality to be small for small angles of θ . Effects of sample shape on the vaporization process have also been estimated by Ward⁸⁸.

There are a number of complications inherent in the experimental Knudsen cell and sample. If the orifice is not located in an infinitely thin wall, then some of the molecules which enter the orifice will not escape but rather will be reflected according to the distribution given by the cosine law (III-5). The calculation of the decrease from the ideal effusion rate was first carried out by Clausing for channel orifices and for non-ideal orifices in general by Freeman and Edwards⁸⁹. The correction term for this effect is called the Clausing factor.

The Knudsen effusion conditions are not truly an equilibrium situation because of continous loss of vapor through the orifice. Displacement from equilibrium may in fact be used to determine if there is a kinetic or thermodynamic barrier to vaporization. Carlson et al. 90 have derived an expression (III-6) to correct the observed pressure, P,

$$P = \frac{P_{eq}}{[1 + (A/a)]}$$
 (III-6)

to the equilibrium value, P_{eq}, <u>i.e.</u> the value at zero orifice size. In equation (III-6) A is the ideal orifice area and a is the sample area. Deviations from relationship (III-6) between observed and equilibrium pressures are usually due to a diffusion barrier or a small evaporation coefficient (defined as the ratio of the Langmuir to Knudsen pressures).

Balson⁹¹ and Carlson et al.⁹⁰ have considered the consequences of cell geometry on the total rate of effusion and they note that the effects are generally small. Errors in vapor pressure measurements which result from temperature gradients in a Knudsen cell have been described by Storms⁹².

The limitations of experimental systems frequently make it very difficult to measure the individual contributions of the various deviations from the ideal effusion experiment. System parameters are optimized so as to minimize the magnitudes of the deviations and no corrections are made. The ideal equilibrium vapor pressure, P, in a Knudsen effusion experiment is given by (III-7) where W is the mass of

$$P = \left(\frac{W}{At}\right) (2\pi RT/M)^{1/2}$$
 (III-7)

the effusate of molecular weight M passing through an orifice of area A in time t.

b. Target Collection

The effusion rate can be determined by measuring the momentum of the effusing molecules (torsion effusion) or the number of effusing

molecules and their mass (weight-loss experiment). Alternatively, a known fraction of the effusate may be collected and from this, the total rate of effusion and hence the pressure determined.

The fraction of molecules striking a circular collector plate of radius r, the center of which is coaxial with the normal to the orifice and at a distance d from it may be calculated from the cosine law (III-5). Equation (III-7) may be restated for target collection (III-8) with P in

$$P = \frac{3.76 \times 10^{-4} \text{ W}}{\text{At}} (T/M)^{1/2} [(d^2 + r^2)/r^2]$$
 (III-8)

atm, t in min, A in cm², and W in g.

In this equation it is assumed that all effusing molecules striking the collector plate adhere. An advantage of a target collection experiment is that the correction for non-ideality of conical orifices is generally small since only the fraction of the effusate within a small solid angle ($d\omega$) from the normal is collected.

c. Analysis of the Collected Effusate

The fraction of the effusate collected on a target can be analyzed by chemical, electrochemical, X-ray fluorescence, or radiochemical techniques often with a greater sensitivity than is possible by measuring the mass gained by the target.

Parrish⁹³ has described the use of secondary or fluorescent X-rays for quantitative analysis. The fluorescent X-ray arises from radiation which is emitted when an inner electron vacancy is filled by an outer electron. The energy of this X-ray is characteristic of the particular transition for that element. Since these transitions are nearly independent of the chemical environment, the X-ray fluorescence technique can be used conveniently for elemental analyses without the need to know the chemical form of the element.

Submicrogram levels of the lanthanides may be analyzed using neutron activation analysis (NAA) since nearly all lanthanide nuclides have high capture cross-sections for thermal neutrons⁹⁴. After neutron irradiation of a sample, induced radiation may be counted and used as a quantitative or qualitative measure of the lanthanide present. Again, the chemical environment of the sample is of little consequence since the emitted radiation is predominantly characteristic of the particular nuclides produced by irradiation.

d. Temperature Measurement

Temperature may be measured with an optical pyrometer by comparing the intensity of light from a standard lamp with the intensity of light radiating from a hot object. The basic principle involved is Planck's quantum relationship of the intensity and wavelength of radiation by a blackbody⁹⁵. Corrections must be applied for absorption and reflection of light by the optical elements in the system. The transmissivity, τ , of each optical element reduces the apparent temperature according to the relationship⁹⁶ given by equation (III-9) where T_a is the apparent

$$\frac{1}{T_a} - \frac{1}{T_t} = \frac{\lambda_e(T_a, T_t) \ln \tau}{c_2} = \frac{\lambda_1}{T}$$
 (III-9)

temperature, T_t is the true blackbody temperature, λ_e is the effective wavelength of the pyrometer in the interval from T_a to T_t , and $c_2 = hc/k = 1.438$ cm deg which is the second fundamental radiation constant. Since the pyrometer generally operates over only a small wavelength region through the use of filters, $\Delta \frac{1}{T}$ is nearly temperature independent. That the values of $\Delta \frac{1}{T}$ for the various optical elements are additive is a consequence of Beer's law which states that equal fractions of the incident radiation are transmitted by equal changes in the path

length of the absorbing substance.

e. Identification of Vapor Species

The nature of the effusing vapor must be determined for characterization of the reaction and for effusion rate calculations. The mass spectrometer is used extensively for such identifications. Indeed, if the sensitivity of the mass spectrometer can be calibrated in absolute pressure units, it could be used for the total Knudsen effusion experiment.

The principle of operation of a time-of-flight mass spectrometer designed for Knudsen studies as described by Pilato⁹⁷ involves the imparting of equal kinetic energy to all the singly ionized species in the source region of the instrument. These species are then permitted to drift in a field free region to produce velocity discrimination. Since the velocity squared is inversely proportional to the mass of the species, mass separation is effected.

4. Thermodynamic Calculations

Under the experimental conditions of a Knudsen vaporization alluded to earlier, the vapor pressure must be much less than one atmosphere so that the vapor may be considered an ideal gas and the activities of the species in the vapor can be taken as their partial pressures. Equilibrium constants of reactions of interest may be obtained from products of activities, and enthalpies and entropies may be obtained from the variation of the equilibrium constants with temperature.

a. Second Law Method

The standard free energy change, $\Delta G_{T}^{\circ},$ for a reaction at temperature, T,

is given by equation (III-10) where K is the equilibrium constant.

$$\Delta G_{T}^{\circ} = -RT \ln K = \Delta H_{T}^{\circ} - T \Delta S_{T}^{\circ}$$
 (III-10)

Inherent in the use of partial pressures for equilibrium constant calculations is the assumption that the activity of all condensed phases is unity. This assumption is probably valid in the case of a congruent vaporization but should be examined more critically for an incongruent process. Rearrangement of equation (III-10) to the usual form of an equation of a straight line (III-11) allows the enthalpy, ΔHT , and

$$\ln P = -\Delta H_{T}^{\circ} + \Delta S_{T}^{\circ}$$
(III-11)

entropy, ΔS_T^{\bullet} , of reaction to be obtained from the slope and intercept respectively.

Experimental data are usually considered in the form of a log P versus (1/T) plot and the best straight line is fit to the data by a least squares technique. The enthalpy and entropy of reaction are assigned to the median temperature of the experiment. Frequently the plot is linear within experimental uncertainty. This assumption of linearity implies that the change in heat capacity is constant over the measured temperature range.

If the heat capacities of the reactants and products are known or can be estimated, the thermochemical values for the experimental median temperature, T_m , may be expressed at a reference temperature, T_r , by means of equations (III-12) and (III-13).

$$\Delta H_{T_m}^{\bullet} = \Delta H_{T_r}^{\bullet} + \int_{T_r}^{T_m} \Delta C_p dT$$
 (III-12)

$$\Delta S_{T_m}^{\circ} = \Delta H_{T_r}^{\circ} + \int_{T_r}^{T_m} \frac{\Delta C_p}{T} dT \qquad (III-13)$$

The term ΔC_p is the heat capacity difference between the products and reactants.

b. Third Law Method

The availability of spectroscopic data and determined heat capacities permits computation of free energy data as a function of temperature. These smooth functions, free energy functions (fef), as defined in equation (III-14) for a temperature, T_r , and a reference temperature, T_r ,

$$fef_{T} = (G_{T}^{\circ} - H_{T_{r}}^{\circ})/T$$
 (III-14)

are conveniently extrapolated with a high degree of precision. They provide a check of the second law enthalpy and allow direct comparison of data from different sources. This function can be calculated directly for gases when the spectroscopic energy levels are known⁹⁸.

Equation (III-14) may be restated as (III-15) by using (III-10).

$$fef_{T} = (H_{T}^{\circ} - H_{T_{r}}^{\circ})/T - S_{T}^{\circ} = (H_{T}^{\circ} - H_{T_{r}}^{\circ})/T - (S_{T}^{\circ} - S_{T_{r}}^{\circ}) - S_{T_{r}}^{\circ} (III-15)$$

For a reaction Δ fef is the difference between the fef of the products and that of the reactants and may also be expressed as (III-16). The

$$\Delta fef = - \Delta G_{T}^{\circ} + \Delta H_{T_{r}}^{\circ}$$
(III-16)

enthalpy of reaction at the reference temperature is then give by (III-17).

$$\Delta H_{T_r}^{\circ} = -RT \ln P + T \Delta f e f \qquad (III-17)$$

Equilibrium data may be treated by the third law method by calculating $\Delta H_{T_r}^{\circ}$ or ΔH_{T}° directly from each experimental datum point with tabulated, calculated, or estimated entropies or free energy functions and equations (III-17) or (III-18).

$$\Delta H_{T}^{\circ} = -RT \ln P + T \Delta S_{T}^{\circ}$$
 (III-18)

The third law method is used commonly to test for systematic errors in the measured temperatures or pressures. A temperature dependent trend in the third law enthalpy values is indicative of some systematic error present in the experiment or the free energy function used. On the other hand, disparity between the second and third law enthalpy values may indicate an error in the definition of the vaporization process or a vaporization coefficient (III-A-3-a) that deviates greatly from unity.

c. Sources of Thermodynamic Data

Compilations of thermodynamic data are available from a number of sources⁹⁹. However, some of the necessary information frequently is not available and must be estimated. Various techniques for estimating these data have been reviewed by Stull and Prophet^{100,101}.

B. Structural Determination

The solution of a crystal structure by diffraction methods can be separated into two parts. The first is concerned with determination of the size, shape, and symmetry of the crystal lattice from a diffraction pattern. The second is the obtaining of diffracted intensity data which can be related to the distribution of the scattering material (the electrons in the case of X-ray diffraction) within the lattice.

1. Unit Cell Determination

In general many properties of a crystal are not the same in all directions. The variation in properties with direction is a consequence of the regular packing of the atoms in the crystal and is of importance in a structural determination. The shape of a crystal is not a fixed characteristic of the substance but is dependent upon the

conditions of crystal growth and thus the morphological determination of the unit cell by optical techniques is frequently restricted by practical considerations.

a. Optical Properties

For monochromatic light cubic crystals are isotropic while all non-cubic crystals divide an entering ray into two polarized rays at least one of which is dependent upon the direction of propagation, that is, birefringence. The certain directions where deviation of the entering ray does not occur are called the optic axes¹⁰². Birefringence may be used to advantage by examining a crystal under crossed polarizing analyzers and determining the optical extinction axes. Tetragonal, hexagonal, and trigonal crystals are uniaxial, while orthorhombic, monoclinic, and triclinic crystals are biaxial. Thus optical examination can be used to determine the crystal system of transparent crystals. In general an optical axis is coaxial with a crystallographic axis.

b. Symmetry Elements and Systematic Absences

The intensity of an X-ray reflection depends upon the distribution of electrons in the crystal. Absent reflections which are randomly distributed among the possible indices are due to low electron density. Sometimes the absent reflections are systematically distributed and can be related to the presence of symmetry elements in the crystal. If the structure factor expression (III-19) where f_n is the atomic scattering

 $F(hkl) = \sum_{n} f_n \exp \left[2\pi i (hx_n + ky_n + lz_n)\right] \qquad (III-19)$ factor, (x_n, y_n, z_n) are the coordinates of atom n, and (h, k, l) the Miller indices, is used to represent the directionalized scattering, the source of systematic absences can be considered. The summation is to be taken over all atoms in the cell. If there are no relations among the

various atomic coordinates, the expression cannot be simplified.

However, if there is some relationship among the positions, equation

(III-19) may be simplified by collecting into a group those atoms

that form a related set. If the relationship arises from a translational

symmetry element, the structure factor will be zero for a systematic set

of (hkl). The conditions for systematic absence of reflections for

the various translational symmetry elements are given by Henry and

Lonsdale 103.

c. Unit Cell Axial Lengths and Space Group

The axial lengths can be deduced from measurements of the diffraction data. The diffraction record is a picture of the reciprocal lattice which describes completely the direct lattice of the crystal. The optical and X-ray diffraction information can be utilized to determine the space group to which the crystal belongs¹⁰⁴. Unfortunately, due to the center of symmetry introduced by the X-ray diffraction phenomenom itself, only translational symmetry elements are detected and these may not uniquely determine the space group.

d. Density Measurements

Combination of density measurements and dimensions of the unit cell will give a value of the total formula weight of the cell contents. From this weight it is usually possible to deduce the number of asymmetric units in the unit cell. The density, ρ , of a crystal may be determined from a comparison of the weight of the sample in a fluid of known density, D, with its weight in air according to (III-20).

$$\rho = [W_{air}/(W_{air} - W_{fluid})] \times D_{fluid}$$
 (III-20)

2. Intensity Data Collection

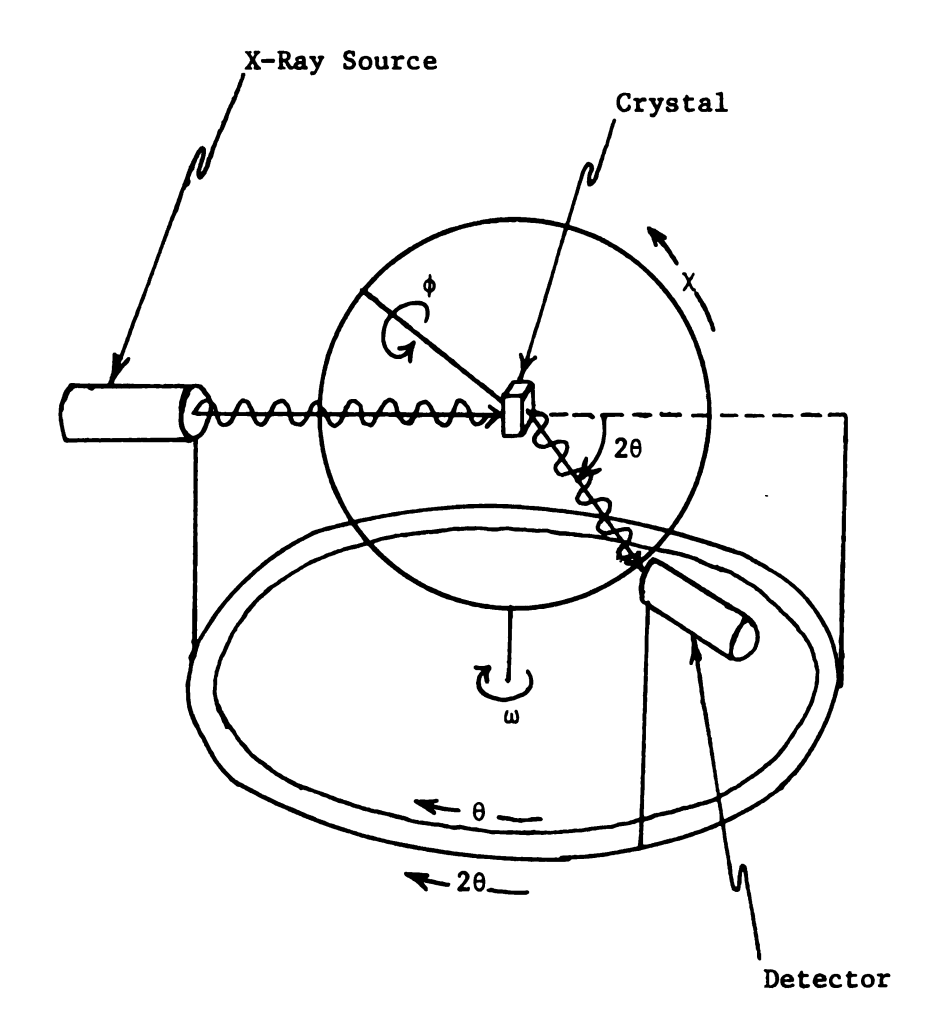
a. Eulerian Geometry Diffractometer

There are two basic geometrical configurations which have been utilized in the construction of single crystal diffractometers - the equi-inclination and the normal beam setting. In equi-inclination geometry, upper level reflections are measured by tilting the detector while in the normal beam method, the crystal rather than the detector is tilted.

Furnas and Harker¹⁰⁵ described a normal beam system which permits the detector to rotate only about a vertical axis while the crystal is oriented by rotation about three axes. This crystal support system is called an Eulerian cradle because it permits rotation about each of the Eulerian axes. A diagram of a four-circle Eulerian cradle is given in Figure 1. The positive sense of each of the axes as indicated is for a left-handed system.

The ϕ - circle is carried on the χ - circle which in turn is carried on the ω - circle. The entire cradle goniostat is mounted on the θ - circle of the diffractometer. The θ - 20 relationship necessary for satisfaction of the Bragg diffraction geometry is maintained by the diffractometer table. To measure the intensity of a reflection, the crystal is adjusted by manipulating the φ , χ , and ω - circles so that the reciprocal lattice point corresponding to the reflection is brought into the zero level with respect to the vertical ω - axis. When the cradle is used in the three-circle mode, the ω - circle is fixed with respect to the θ - circle.

FIGURE 1. A Four-circle Normal Beam Eulerian Cradle



b. Eulerian Axes

Use of a three- or four-circle X-ray diffractometer requires a knowledge of the size, shape, and orientation of the unit cell. The size and shape of the unit cell are initially most conveniently determined using film techniques although the diffractometer is suited for the precise determination of roughly known lattice constants. The orientation problem is one of fixing the position of the unit cell coordinate system relative to the axes of the diffractometer. The problem is the same as that of describing the rotational motions of a rigid body relative to a set of axes, the orientation of which is fixed in space.

A number of systems have been used to describe the transformation between the two coordinate systems; a common one uses the Eulerian angles. The description which follows is based upon one of the coordinate systems being right-handed and the other left-handed.

This choice is necessitated by the construction of the Siemens Eulerian cradle used in this investigation and the usual right-handed specification of crystal lattices. The more common situation of a transformation from one right-handed system to another right-handed system is described by Goldstein 106.

If one of the coordinate systems is rigidly attached to the body (the crystal being examined), six parameters are necessary and sufficient to give the explicit relationship between the coordinate systems. Three of the parameters specify a fixed point in the body, two more are required to define the position of a line fixed in the body and passing through the fixed point and the sixth parameter defines a rotation of the body about this line. If the two coordinate systems are taken to

have a common origin, the Eulerian angles as shown in Figure 2 are defined as follows:

- α is the angle resulting from rotation of the initial set of axes OABC about the z-axis OZ.
- β is the angle obtained by rotating OC about the intermediate axis OK until it is in coincidence with OZ.
- γ is the angle of rotation about OZ which brings OA to OX and OB to OY.

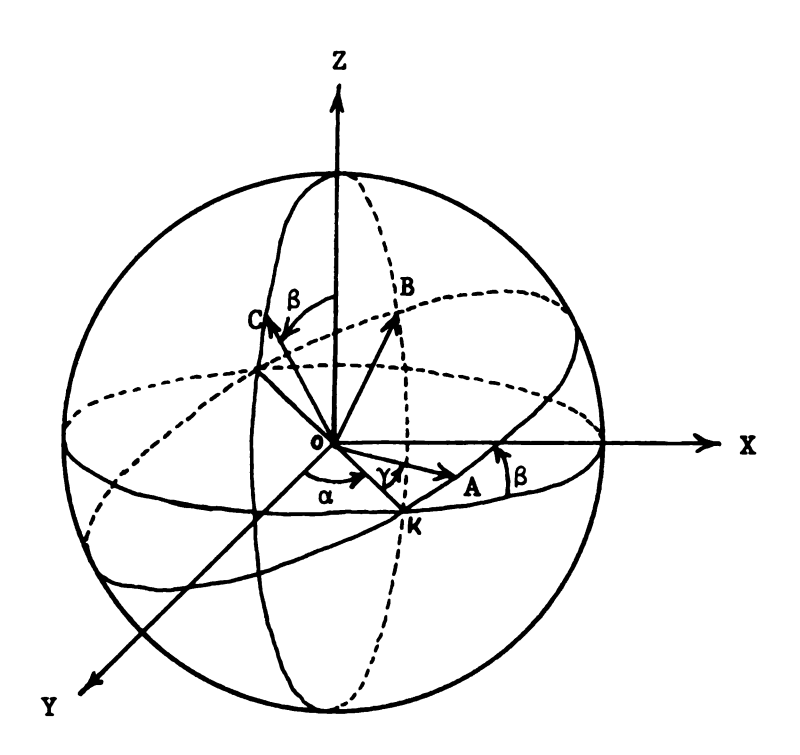
These operations must be performed in the sequence given. The relationship between OABC and OXYZ may be obtained by projecting the direction cosines of OX, OY, and OZ and then defining them in relation to the direction cosines of OA, OB, and OC. For example, $\cos \alpha$ becomes $\cos \alpha$ sin β along OZ and $\cos \beta$ becomes $\cos \alpha$ $\cos \beta$ $\cos \gamma$ along OX. The complete transformation matrix is given below.

The determination of the orientation in actual practice is effected with the aid of computer program B-101 described in Appendix II.

c. Crystal Monochromator

Limiting factors in the obtaining of an accurate intensity record in a single crystal study are background radiation and the varying resolution of the $K_{\alpha 1}$ - $_{\alpha 2}$ doublet of the filtered incident radiation. The use of a crystal monochromator provides the most satisfactory solution available today for these problems.

FIGURE 2. Eulerian Axes.



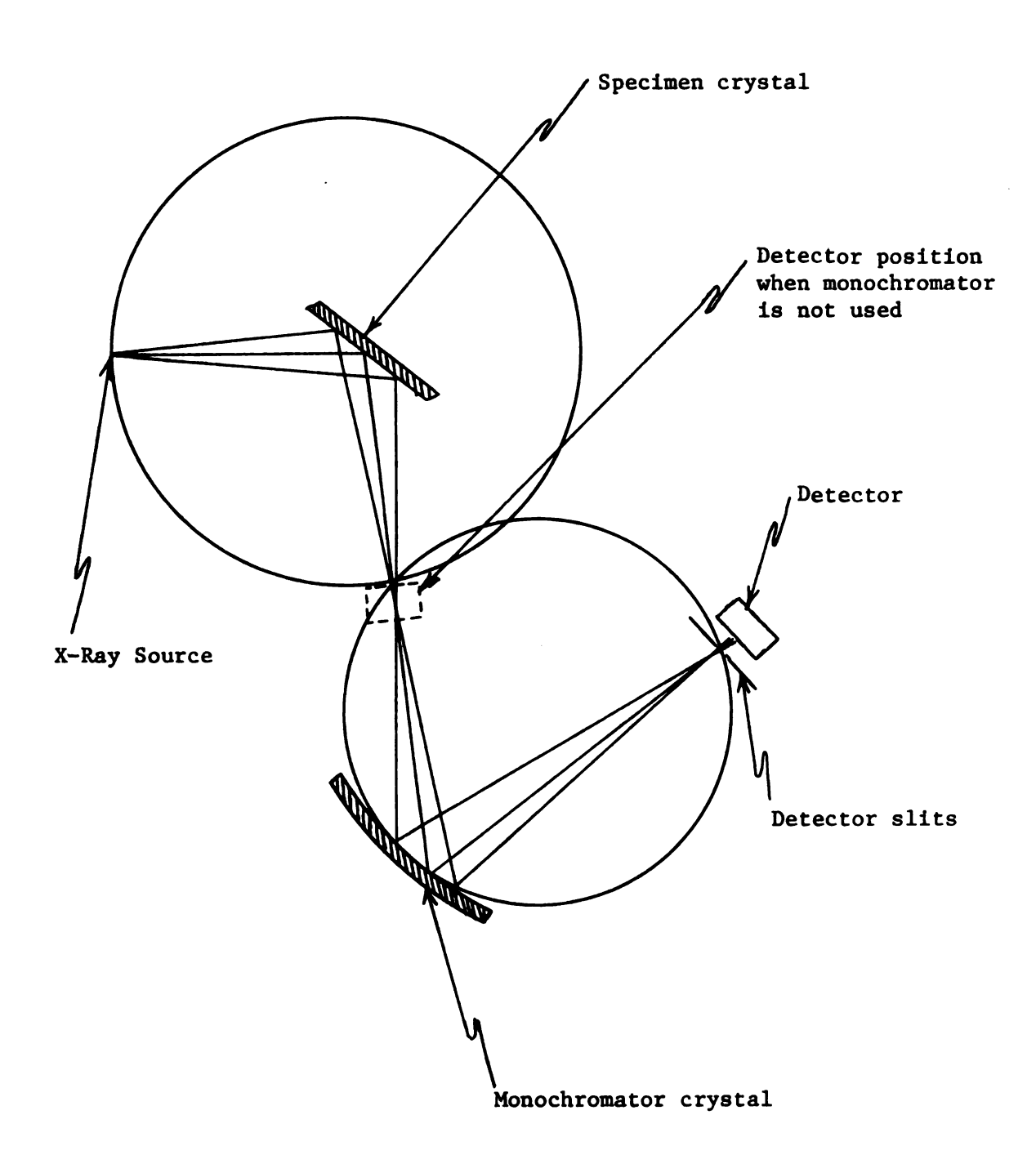
The monochromator used in this work is based on the X-ray optics developed by Johannson¹⁰⁷. Figure 3 gives a ray diagram of the diffractometer and monochromator optics. The X-rays are diffracted by a quartz plate which is cut parallel to the plane (1011), cylindrically ground to a radius of 2r, and elastically bent to a radius of r. For this geometry the monochromator source (the detector slit of the diffractometer), the surface of the monochromator crystal and the monochromator exit all lie on the focussing circle whose radius is r.

d. Intensity Data Collection Techniques

For a structural determination the integrated intensity of a reflection, a quantity proportional to the total energy diffracted by the crystal as it passes through the Bragg reflecting position, must be obtained. The observed intensity is related to the integrated intensity by a number of geometrical and physical factors which will be considered in (III-B-3).

There are three measuring procedures which may be used to collect the various reflection intensities with an Eulerian cradle set in normal beam geometry. These are the stationary crystal-stationary detector method, the moving crystal-stationary detector method (ω - scan), and the moving crystal-moving detector method ($\omega/2\theta$ - scan). Under ideal conditions with strictly monochromatic radiation there is little difference among the accuracies obtained with the three methods. In actual practice the preferred technique¹⁰⁸ would be combination of the ω - scan and the $\omega/2\theta$ -scan depending upon the region of reciprocal space being explored. The various systematic errors introduced by each of these methods has been considered by Furnas¹⁰⁹.

FIGURE 3. Diffractometer and Monochromator Optics.



3. Data Reduction

The ultimate aim in a structural determination is to relate the electron density distribution calculated for the model being used to describe the crystal to the measured intensities. From the observed intensities only the absolute amplitudes of the structure factors (III-19) may be determined.

a. Geometrical Factors

(1) Polarization Factor

The polarization correction arises because the efficiency of reflection of the X-ray beam varies with reflection angle. The incident unpolarized beam may be described in terms of two electric vectors, one parallel to the reflecting plane and the other normal to it. The intensity at any point from an X-ray scattered by an electron is proportional to the angle between the incident radiation and the direction in which the scattering electron is accelerated 110 . Waves having their electric vector parallel to the reflecting plane are reflected to an extent determined by the electron density, while those having their electric vector perpendicular to the plane are scattered to an extent dependent upon both the electron density and scattering angle. The overall polarizing factor, p, is a function of only the reflection angle, θ , and is given by (III-21).

$$p = \frac{1 + \cos^2 2\theta}{2} \tag{III-21}$$

(2) Lorentz Factor

The intensity of a reflection is proportional to the time during which the corresponding reciprocal lattice point is close to the surface of the reflecting sphere. The Lorentz factor corrects for the different rates at which reciprocal lattice points sweep through

the sphere boundry and thus is dependent upon the experimental arrangement. For the normal beam method (reflecting planes parallel to the rotation axis) the angular velocity is dependent only upon the angle between the tangent to the surface of the reflecting sphere and the path of the reciprocal lattice point. This angle, θ , is the Bragg angle¹¹¹. The Lorentz factor, L, is given by (III-22).

$$L = \frac{1}{\sin 2\theta} \tag{III-22}$$

(3) Monochromator Factor

The monochromator correction term is also a polarization correction. However, in this case the incident radiation is partially polarized due to diffraction by the crystal. The form of the correction, m, is given 112 by (III-23) where $\theta_{\rm m}$ is the Bragg angle of the monochromator

$$m = \frac{1 + \cos^2 2\theta_m \cos^2 2\theta}{1 + \cos^2 2\theta_m}$$
 (III-23)

b. Physical Factors

(1) Absorption

X-Rays are absorbed as well as scattered in their passage through matter. The change in intensity, dI, of the original intensity, I, is given by (III-24) where t is the sample thickness and μ is the linear

$$- \underline{dI} = \mu dt$$
 (III-24)

absorption coefficient. The linear absorption coefficient of a crystal may be computed from a knowledge of its chemical composition, its density, and a table of mass absorption coefficients¹¹³ by (III-25) in which

$$\mu = \rho \sum_{\mathbf{n}} \mathbf{w}_{\mathbf{n}} \mathbf{a}_{\mathbf{n}} \tag{III-25}$$

 $\mathbf{w_n}$ is the weight fraction of element n in the compound, $\mathbf{a_n}$ is the mass absorption coefficient of n for the radiation employed, and ρ is the

crystal density.

The absorption calculation must be carried out separately for each reflection since it depends upon the paths of the incident and diffracted beams through the crystal.

(2) Extinction

An ideally perfect crystal is composed entirely of a single sequence of planes in a perfect array. In such a crystal the diffracted beam is at the Bragg angle to be reflected back to the direct beam with resulting destructive interference. This effect, known as primary extinction, appears as enhanced absorption along the direction of Bragg reflection. The net result of these interferences from multiple reflections is to cause the intensity of the diffracted beam to be proportional to $|F_{hk\ell}|$ and not $|F_{hk\ell}|^2$. An ideally imperfect crystal is composed of mosaic blocks so small that within each one primary extinction does not occur to an appreciable amount.

Secondary extinction results from reduction of the intensity of the incident beam by Bragg reflection. Successive planes in identically aligned mosaic blocks receive an attenuated beam even if there is no primary extinction.

Because of the difficulty of describing the "perfectness" of a crystal, the factor upon which extinction is dependent, these corrections are usually effected on an empirical basis.

4. Solution of the Structure

The experimentally obtained diffraction intensities contain only part of the information necessary for solution of the structure. The part which cannot be obtained experimentally is the phase of the scattered radiation which is contained in the exponential part of (III-19). The

supplying of this missing information for which no general method has been found is the so-called "phase problem" of structural determination.

a. Fourier Synthesis

A periodic function such as the electron density distribution in a crystal can be represented by a summation of sine and cosine terms called a Fourier series. The structure factor (III-19) may also be expressed (III-26) as the sum of the wavelets from all the infinitesimal volume

$$F_{hkl} = \int_{V} \rho(x,y,z) \exp[2\pi i(hx + ky + lz)] dV \qquad (III-26)$$

elements of electron density, $\rho(x, y, z)$ dV, where V is the cell volume. The exponential part of (III-26) may be written in the form of a trigonometric function and thus may be stated as a Fourier series (III-27)

$$F_{hk\ell} = \int_{V} \sum_{h} \sum_{k} \sum_{\ell} C_{\overline{hk\ell}} \exp \left\{2\pi i \left[(h+h')x + (k+k')y + (\ell+\ell')z \right] \right\} dV$$
(III-27)

where the C terms are the coefficients in the series such that after integration over all terms equation (III-28) results.

$$F_{hk\ell} = \int_{V} C_{\overline{hk\ell}} dV = VC_{\overline{hk\ell}}$$
 (III-28)

The relationship between the electron density, ρ , and the structure factors, F, is that one is the Fourier transform of the other (III-29)

$$\rho(\mathbf{x},\mathbf{y},\mathbf{z}) = \frac{1}{V} \sum_{\mathbf{h}} \sum_{\mathbf{k}} \sum_{\mathbf{l}} \mathbf{F}_{\mathbf{h}\mathbf{k}\mathbf{l}} \exp[-2\pi \mathbf{i}(\mathbf{h}\mathbf{x} + \mathbf{k}\mathbf{y} + \mathbf{l}\mathbf{z} - \alpha_{\mathbf{h}\mathbf{k}\mathbf{l}})] \quad (\text{III}-29)$$

where $\alpha_{hk\ell}$ is the phase angle

$$\alpha_{hkl} = \tan^{-1} \left(\frac{\sum_{f} \sin 2\pi (hx + ky + \ell z)}{\sum_{f} \cos 2\pi (hx + ky + \ell z)} \right)$$
(III-30)

b. Patterson Synthesis

The experimentally unobtainable phases prohibit the use of (III-29) for the direct solution of the structure. The Patterson function 114 is a form of Fourier series employing $|F_{hkl}|^2$ which does not depend upon

phases. If the phases were available, the usual Fourier synthesis would show the distribution of atoms in the cell; the $|F|^2$ Patterson synthesis has peaks corresponding to all the interatomic vectors in the cell. The Patterson function (III-31) has certain properties 114 which may be used to relate the interatomic vectors to atomic positions. The Patterson

$$A(x,y,z) = \frac{1}{v} \sum_{h} \sum_{k} \sum_{\ell} |F_{hk\ell}|^2 \cos 2\pi (hx+ky+\ell z)$$
 (III-31)

function is centrosymmetric and as a result all translational symmetry elements in the space group are replaced by their corresponding non-translational elements.

Although the translational symmetry elements do not appear, symmetry related atoms produce a concentration of vectors in certain planes called Harker sections. Even though there are ambiguities in their interpretation, the Harker sections frequently can be used to determine the heavy atom position in the cell. Once the heavy atom position is known, it is practical to use a synthesis of the type (III-29) or variations of it since the scattering phases are dominated by the heavy atom. Location of other atoms should proceed rather directly from this point 115.

c. Least-Squares Refinement

The least-squares structure refinement consists of systematically varying the atomic parameters to minimize the function R (variously called the reliability or residual factor) as defined in (III-32) where

$$R = \frac{\sum ||F_{O}| - |F_{C}||}{\sum |F_{O}|}$$
 (III-32)

 $\mathbf{F}_{\mathbf{O}}$ and $\mathbf{F}_{\mathbf{C}}$ are respectively the observed and calculated structure factors.

(1) Thermal Parameters

A succeeding stage in refinement of a structural model is to introduce a thermal parameter for each atom. The scattering power of

a real atom (f_n in equation (III-19)) decreases with increasing $\sin \theta/\lambda$ because of the distribution of electrons about the nucleus. Further, such distribution is based upon atoms at rest at their lattice points. The fact that real atoms vibrate has the effect of dispersing the electron cloud over a larger volume of space. As a consequence, the effective scattering power decreases faster than that for a stationary atom. The correction term to the scattering factor for this effect is given by (III-33) where B is the thermal parameter and is related to the mean

$$e^{-B(\sin^2\theta/\lambda^2)} = \exp\left[\frac{-B}{4}(1/d_{hk\ell})^2\right]$$
 (III-33)

square amplitude of the atomic vibration, $\overline{u^2}$, by relationship (III-34).

$$B = 8\pi^2 \overline{u^2}$$
 (III-34)

A further refinement is to allow the model to vibrate anisotropically and for this case (III-33) becomes (III-35).

exp [
$$-(\beta_{11}h^2 + \beta_{22}k^2 + \beta_{33}l^2 + 2\beta_{12}hk + 2\beta_{13}hl + 2\beta_{23}kl)$$
] (III-35)

(2) Anomalous Dispersion

Although the atomic scattering factor, f_n , has heretofore been treated as a real number, the scattering phenomenon in fact introduces a phase change which requires the scattering factor to be represented by a complex expression (III-36) in which ($\Delta f' + i\Delta f''$) are the anomalous

$$f_n^{corr} = f_n + (\Delta f' + i\Delta f'')$$
 (III-36)

dispersion correction terms. These terms are relatively independent of $\sin \theta/\lambda$.

CHAPTER IV

EXPERIMENTAL MATERIALS, EQUIPMENT, AND PROCEDURES

A. Materials

Chemicals and materials used were: (a) chlorine, 99% purity,

(b) hydrogen chloride, 96%, (c) argon, 99.8% (d) ultra-pure hydrogen,

99.9+%, Matheson, Joliet, IL (e) helium, 99.9% (f) hydrochloric acid,

reagent (g) nitric acid, reagent (h) silver nitrate, reagent (i) thionyl

chloride, reagent (j) anhydrous ammonium chloride, reagent (k) carbon

tetrachloride, reagent (l) chloroform, reagent (m) 1,2-dibromoethane,

reagent (n) zinc metal, 40 mesh, reagent (o) ytterbium metal, distilled

ingot, 99.9%, Research Chemicals, Phoenix, AZ (p) Yb203, Tm203, Lu203,

Ho203 and Dy203, 99.9% lanthanide purity, Michigan Chemical, St. Louis,

MI (q) Thoria, 99%, Zirconium Corporation, Solon, OH (r) graphite stock,

spectroscopic grade, National Carbon, Bay City, MI (s) quartz, 99.9%

(t) molybdenum stock, Kulite Tungsten, Ridgefield, NJ.

B. Sample Preparation

1. Ytterbium Trichloride Hexahydrate

Ytterbium trichloride hexahydrate was prepared by dissolution of Yb₂O₃ in concentrated hydrochloric acid. The solution was evaporated to dryness at 80°.

2. Ytterbium Trichloride

Six different chlorinating agents were tried in the preparation of anhydrous YbCl₃. The starting material for these preparations was either

the calcined sesquioxide or the hydrated trichloride obtained as in (IV-B-1) above except that the solution was evaporated to dryness at 120°. The crude YbCl₃ product obtained by the methods described below was purified by sublimation. The sample contained in a quartz boat was sublimed at 700° under a chlorine atmosphere and collected on the cooler walls of the tube furnace apparatus.

a. Thionyl Chloride

An argon gas stream was used to sweep $SOC1_2$ over heated Yb_2O_3 in an attempt to repeat the preparation of pure $YbC1_3$ described by Machlan et al.³⁵ as taking place according to equation (IV-1).

$$Yb_2O_3(s) + 3SOCl_2(l) = 2YbCl_3(s) + 3SO_2(g)$$
 (IV-1)

This preparation was attempted at reaction temperatures maintained between 410° and 550°. The reaction period was approximately four hours at the maximum temperature for the experiment.

b. Chloroform

A single preparation using CHCl₃ swept in an argon stream over the heated hydrated trichloride starting material was effected for two hours at 600°.

c. Carbon Tetrachloride

The reaction of CCl_4 with lanthanide sesquioxides is reported to occur in accordance with equations (IV-2) and (IV-3)⁹. These reactions were

$$Ln_2O_3(s) + 3CCl_4(l) = 2LnCl_3(s) + 3Cl_2(g) + 3CO(g)$$
 (IV-2)

$$Ln_2O_3(s) + 3CCl_4(l) = 2LnCl_3(s) + 3COCl_2(g)$$
 (IV-3)

studied by carrying CCl $_4$ with an argon flow over Yb_2O_3 heated to 550-700° for a period of several hours.

d. Chlorine

The direct reaction of chlorine gas with the heated hydrated

trichloride starting material was conducted at temperatures up to 900° for intervals up to 18 hours.

e. Hydrogen Chloride

Hydrogen chloride or hydrogen chloride diluted with helium or argon was used as the chlorinating agent in preparations using either of the described starting materials. Preparations were conducted at sample temperatures in the range of 500 to 850°. The reaction period was usually dictated by malfunction of the hydrogen chloride flow regulating equipment.

f. Ammonium Chloride

A six-fold excess of ammonium chloride was coprecipitated with the hydrated trichloride. The ammonium chloride-ytterbium chloride mixture was air-dried for several days at 120° and then transferred to a quartz tube or graphite crucible. In each case the mixture was heated slowly in vacuo to 350°. The heating rate was adjusted to allow removal of water before the excess NH₄Cl was sublimed away at 350°. The overall reaction is described by (IV-4). The product was ultimately heated to at least

 $Yb_2O_3(s) + 6NH_4C1(s) = 2YbCl_3(s) + 3H_2O(g) + 6NH_3(g)$ (IV-4) 500° before terminating the preparative experiment.

3. Ytterbium Dichloride

a. Metallothermic Reduction

Sublimed YbCl₃ was transferred to a quartz tube to which was added either a stoichiometric amount of ytterbium metal or a two-fold excess of zinc metal according to reactions (IV-5) and (IV-6) respectively. The

$$2YbCl3(s) + Yb(l) = 3YbCl2(s)$$
 (IV-5)

$$2YbCl3(s) + Zn(l) = 2YbCl2(s) + ZnCl2(g)$$
 (IV-6)

tube was evacuated and the sample region was heated in the flame of an oxygen-gas torch. Heating was continued until the excess zinc distilled

from the hot zone and formed a mirror on the cold wall or until the green product distilled from the hot zone.

b. Thermal and Hydrothermic Reduction

A second technique used for preparation of YbCl₂ was to heat YbCl₃ prepared in a graphite crucible as in (IV-B-2-f) in situ to red heat either in vacuum or under approximately a half atmosphere of hydrogen for an hour.

4. Ytterbium Oxidechloride

Thermal decomposition of YbCl₃·6H₂O at 500-600° under an inert atmosphere was used to effect preparation of YbOCl. The decomposition reaction is given in equation (IV-7). Other YbOCl preparative techniques

YbCl
$$_3 \cdot 6H_2O(s) = YbOCl(s) + 5H_2O(g) + 2HCl(g)$$
 (IV-7) included the heating of equimolar amounts of Yb $_2O_3$ and YbCl $_3$ at up to 1100° under both chlorine and inert atmospheres and the direct combination of Yb $_2O_3$ and Cl $_2$ in a manner similar to that described in (IV-B-2-d).

5. Other Oxidechlorides

a. Triytterbium Tetraoxidechloride

Two preparations of Yb₃0₄Cl were attempted. Each involved combination of equimolar amounts of ytterbia and YbOCl according to equation (IV-8);

$$Yb_2O_3(s) + YbOC1(s) = Yb_3O_4C1(s)$$
 (IV-8)

the first under an inert atmosphere and the second under a chlorine atmosphere.

b. Mixed Metal Oxidechlorides

The mixed metal oxidechlorides, LnOCl, were prepared by dissolving appropriate proportions of the sesquioxides in hydrochloric acid and then thermally decomposing the hydrated chloride as described in (IV-B-4).

C. Single Crystal Growth

Single crystals of YbCl₂ and YbOCl were grown by adaptations of the preparatory conditions. Ytterbium dichloride was transported <u>in vacuo</u> to the cold lid of the graphite crucible in which YbCl₂ was contained during a melting experiment. Single crystals were selected from the vapor-transported material.

Single crystals of YbOCl were first observed in the downstream end of the quartz boat containing YbOCl powder heated to 1100° under a chlorine gas stream. Additional crystals of YbOCl were prepared by heating to 1150° for periods which varied from a few days to several weeks powdered YbOCl which had been sealed in a quartz ampoule containing one atmosphere of chlorine.

D. Analytical Techniques

1. Chlorine Analysis

Analysis for chlorine was effected by dissolution of the sample in dilute nitric acid and subsequent determination by a standard silver halide gravimetric technique.

2. Ytterbium Analysis

Some ytterbium chloride samples were analyzed for metal content after the gravimetric chloride determination by precipitation of the excess silver with dilute hydrochloric acid, adjustment of the solution pH with sodium hydroxide to the bromcresol green end-point, and precipitation of ytterbium oxalate by addition of saturated oxalic acid solution. The oxalate precipitate was washed, digested, and then carefully ignited with the metal being determined gravimetrically as the sesquioxide. Ytterbium metal content was also determined by direct ignition of other samples to

the sesquioxide.

3. Oxygen Analysis

Oxygen content was determined by difference.

E. Density Measurement

The density of YbCl₂ was determined by the buoyancy technique. The weight of several crystals contained in a platinum mesh basket which was suspended from the balance pan hanger arm was measured both in the argon atmosphere of the glove box and while the basket and crystals were submerged in 1,2-dibromoethane whose temperature had been carefully measured. The density of the dibromoethane immersion medium was extrapolated from published¹⁴² temperature-density data. The density of YbOCl was not determined.

F. X-Ray Techniques

For various operations a Siemens Kristalloflex IV, Norelco XRG 5000, Norelco, and Picker 809B X-ray generators were used. All work was with copper radiation ($\lambda K\bar{\alpha} = 1.54178\bar{A}$) with the exceptions of the fluorescence analyses which used tungsten radiation and a few Debye-Scherrer photographs taken with iron ($\lambda K\bar{\alpha} = 1.9373\bar{A}$) or chromium ($\lambda K\bar{\alpha} = 2.2909\bar{A}$) radiation.

A water-cooled Na(T1)I scintillation detector was used in conjunction with a Siemens Kompensograph scaling unit for all non-photographic recording. Input to the Kompensograph unit could be selected with a pulse height analyzer and a discriminator.

1. Powder Methods

Most samples were subjected to X-ray powder diffraction examination for aid in phase identification. Debye-Scherrer and forward focussing

Guinier-Hägg cameras were employed with Cu $K\overline{\alpha}$ radiation. Sample preparations and film measurements were essentially identical to those described by Haschke⁷⁷ and Stezowski¹⁴³. Platinum powder $(a_0 = 3.9238 \pm 0.0003\text{Å})^{144}$ was used as an internal standard. Diffraction data were reduced with the aid of the linear regression program of Lindqvist and Wengelein¹⁴⁵.

Samples of YbOCl were examined through use of a Materials Research

Corp. high temperature camera mounted on a Siemens goniostat. The sample

was placed on a platinum resistance heater stage, the platinum again

serving as an internal standard for calibration of diffraction angle. The

atmosphere in the high temperature camera was either helium or a rough

vacuum.

2. Single Crystal Methods

a. Optical Examination

Preliminary examination and selection of crystals was made with the aid of a Bausch and Lomb Dyna-Zoom binocular microscope. The microscope was used with a Donnay optical analyzer for the initial determination of optical properties.

Crystals of YbCl₂ were mounted by wedging them into Pyrex capillaries which were subsequently sealed, while YbOCl crystals were mounted to the outside end of the capillaries using Canada Balsam. The optical properties of the mounted crystals were examined with the aid of a Leitz polarizing microscope.

The size of a crystal was determined by measuring it with a calibrated graticule in the eyepiece ocular of the Dyna-Zoom microscope or from photographs taken with a Bausch and Lomb metallurgical microscope equipped with a Polaroid camera attachment.

b. Cameras

An equi-inclination Weissenberg camera was used to obtain oscillation, rotation, and Weissenberg photographs. A variable magnification Buerger Precession camera was used to examine those regions of reciprocal space which were not accessible with the Weissenberg camera without remounting the crystal. The photographs were used for space group determination and for selection of crystals for use in intensity data collection.

c. Eulerian Cradle

A Siemens four-circle Eulerian cradle with motorized ω -drive was mounted on a Siemens goniostat. The cradle was aligned using a technique described by Samson and Schuelke¹⁴⁶ with the aid of a telescope provided with the cradle and a cathetometer.

d. Monochromator

The Siemens Johannson-type crystal monochromator was mounted on the detector carriage and was adjusted for strictly Cu K α_1 ($\lambda\alpha_1 = 1.54051\text{\AA}$) radiation by varying the glancing angle and the edge aperture of the crystal.

e. Crystal Orientation

Mechanical shortcomings of the Siemens goniometer head made it impossible to use the usual method of aligning a crystallographic axis along the ϕ -axis of the cradle. As the crystal was viewed through the detector slits with the cathetometer, it was centered by varying the height and the two translational adjustments. Alignment of the crystal with the X-ray beam was impractical so further work proceeded with the crystal in a random orientation.

The initial set of reflections was detected by setting the 2θ -circle according to the values obtained from powder work and then scanning the χ - and ϕ -circles. While the choice of signs of the crystallographic axes is quite arbitrary except in the case of the determination of the absolute configuration of a non-centrosymmetric crystal, the assignment of signs to the various (hkl) reflections must be done in a consistent manner. An incorrect set of signs is reflected in the inability of the B-101 program to compute the projection of the crystallographic axes upon the cradle axes.

f. Lattice Parameter Refinement

Preliminary lattice parameters were obtained from the linear regression analysis of the powder diffraction data. The refined lattice parameters were determined from diffractometer 2θ values measured for pairs of (hkl) and (hkl) reflections. By determining the angle between the pairs of 2θ positions without changing the χ , ϕ , and ω settings, errors in the zero position of the diffractometer table as well as errors due to absorption and incorrect crystal centering are eliminated 147.

g. Intensity Data Collection

The dead time of the counter and scaling equipment was determined from high count rates obtained from the direct beam with copper foil attenuators. For data collection the stationary crystal-stationary detector method was used.

The stability of the experimental setup was determined by periodically observing during the course of the data collection several reflections designated as standards. Data for each reflection were collected for 20000 counts or four minutes, whichever came first.

3. Fluorescence Methods

The fluorescence equipment consisted of a Siemens 4b nonfocussing spectrometer equipped with a LiF analyzing crystal and a 0.15° Soller slit. The tungsten anode X-ray tube was powered with the Siemens Kristalloflex IV generator.

a. Spectrometer Operation

Optimization procedures described by Neff¹⁴⁸ were used for maximization of sensitivity. Counting and scanning operations developed by Haschke⁷⁷ were used without modification.

b. Spectrometer Calibration

Standard solutions of ytterbium were prepared from Yb₂O₃. Calcined ytterbia samples were weighed with a semi-micro balance, dissolved in a minimal quantity of concentrated HCl, and diluted volumetrically to prepare solutions containing from 37 to 104 µg Yb/ ml.

Standard targets for the preparation of calibration curves were obtained by placing known amounts of the solutions onto targets similar in design and material to those used for collection experiments. Volumetric aliquots were made both by weighing and by use of an ultra precision micro buret (Kontes Glass Co.). The targets were allowed to dry in a desiccator and were then counted using the scanning procedure. A linear calibration curve was obtained from least squares analysis of the number of counts per microgram of Yb.

To allow for shifts in the zero setting of the spectrometer table, the scanning range for each day's operation was determined for a bulk sample of ytterbia from a scan of 20 in the vicinity of the Yb $L\alpha_1$ (λ =1.6719Å) transition.

G. Neutron Activation Analysis

Samples for neutron activation analysis were prepared in a manner similar to that described for the fluorescence targets (IV-F-3-b) except that the solutions were placed on high purity quartz discs. After drying, the samples were calcined overnight and then individually sealed in polyethylene film.

The sample discs along with two blank discs were taken to the University of Michigan's Ford reactor for 24 hours of irradiation at a neutron flux of 8 x 10^{12} n/cm²/sec. The samples were counted for gamma activity on the eighth, tenth, and eleventh days after irradiation.

H. Vaporization Mode Characterization

1. Weight Loss Measurements

Preliminary vapor pressure measurements were made by measuring weight losses which occurred at fixed temperatures through an orifice of known size. By completely vaporizing a sample and measuring the weight loss, an indication of the interaction of the sample with the crucible was obtained.

2. Mass Spectrometric Investigation

A Bendix Time-of-Flight, Model 12, mass spectrometer equipped with a Knudsen source inlet system was employed for determination of the species in the effusate. Crucibles made with channel orifices were heated by radiation and electron bembardment. Electron ionizing beams of up to 75 ev were employed. The appearance potentials of all Yb containing species were obtained by a linear extrapolation technique using mercury and nitrogen as references.

3. Effusate Collection

A quartz cup was inverted over the orifice of a graphite cell containing YbCl₂. When the cell was heated inductively in vacuum a condensable effusate collected in the cup.

4. X-Ray Examination

Solid residues from effusion experiments as well as the condensate collected as described above were examined by X-ray powder diffraction to enable identification of the phases present.

I. Target Collection Technique

1. General Procedure

The effusion-target collection apparatus has been described previously by Kent¹⁴⁹ and Haschke⁷⁷. After the crucible had been heated to red heat and the target magazine cooled, the crucible to target separation was measured with a cathetometer. The cathetometer was used also to ascertain that the crucible was aligned coaxially with the target magazine.

2. Temperature Measurement

Temperature measurements were made with a Leeds and Northrup disappearing filament optical pyrometer. Corrections for prism and window transmissivities were made on the basis of observations of a tungsten strip lamp powered from a constant voltage source. The scale calibration of the pyrometer used for experimental measurements was corrected to the scale calibration of a pyrometer which had been calibrated by the National Bureau of Standards.

3. Orifice Measurement

Areas of effusion cell orifices were determined from photographs

taken with the metallurgical microscope both before and after vaporization experiments. The areas of the photographed orifices were
measured with a compensating polar planimeter. Kent 149 determined
that a correction for thermal expansion of the orifice was not
necessary.

4. Effusion Cell Design

Two types of high density graphite effusion cells as described by Haschke⁷⁷ were used for target collection measurements. In addition, two variations of the symmetrical cell design were used - in one case a tantalum washer was attached to the top surface of the cell and in the other the cell was enclosed in a graphite oven as pictured in Figure 4.

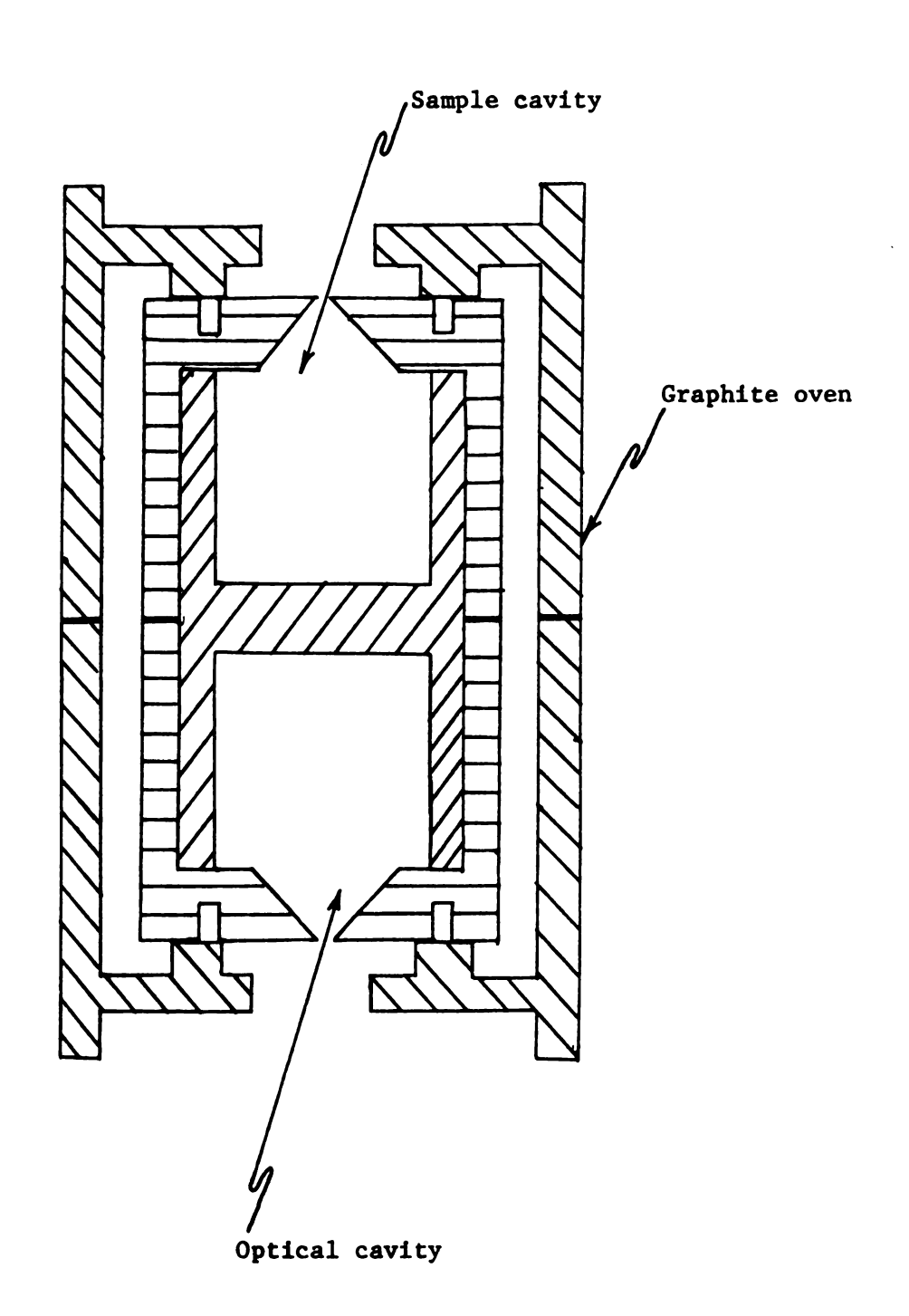
5. Condensation Coefficient Determination

To determine if all the effusate striking a target condenses, the target magazine was fitted with two targets in the following manner: a target of 17.10 mm radius, r_c, which was nearest the effusion cell had an annular hole of 3.12 mm radius, r_b, and was placed 4.85 mm, h, in front of a second target of radius 7.98 mm, r_a. Any effusate after passing through the annular hole which does not condense on the second target is re-emitted with a cosine law distribution. Most of the re-emitted effusate passes back through the annular hole of the first target, but some strikes and condenses on its back. The fraction, f, of re-emitted molecules striking the back of the first target is given by equation (IV-9). If both targets are made from the same material

$$f = \frac{1}{2r_a^2} \{r_c^2 - r_b^2 + [(r_a^2 + r_b^2 + h^2)^2 - 4r_a^2 r_b^2]^{1/2} - [(r_a^2 + r_c^2 + h^2)^2 - 4r_a^2 r_c^2]^{1/2}\}$$
 (IV-9)

and are at the same temperature, the condensation coefficient should be the same for each. On this basis the condensation coefficient may be

FIGURE 4. Effusion Cell Enclosed in Graphite Oven



calculated from measurements of the amount of effusate collected on the second target and the back of the annular target.

J. Auxiliary Equipment

Air sensitive samples were handled in an argon atmosphere glove box which was purged of oxygen and water¹⁴³. The vacuum systems employed for preparations and vaporizations were all cryogenically trapped and evacuated with either silicone oil (DC 704) or mercury diffusion pumps backed by mechanical forepumps. Induction heating was accomplished by coupling the 300kHz output of a saturable reactor controlled Thermonic generator either to the work directly or through a water-cooled copper current concentrator.

CHAPTER V

RESULTS

A. Preparative

Results of elemental analyses are reported in Table I and lattice parameters are listed in Table II. These results are discussed below.

1. Ytterbium Trichloride Hexahydrate

Preparations of YbCl₃·6H₂O yielded small white needle-like hygroscopic crystals. These and all other hygroscopic crystals were manipulated in a glove box and protected by a film of paraffin oil during X-ray powder diffraction examination. Observed interplanar d-spacings and intensities together with values calculated on the basis of the atomic positions reported for GdCl₃·6H₂O are listed in Appendix III-A^{2O}. These data indicate that YbCl₃·6H₂O is isostructural with the other heavy lanthanide trichloride hexahydrates.

2. Ytterbium Trichloride

Preparatory procedures which used SOCl₂, CHCl₃, or CCl₄ were unsatisfactory due to side reactions which produced sulfur, carbon, or hexachloroethane, respectively. The YbCl₃ prepared from ytterbia and chlorine was contaminated with incompletely reacted ytterbia as evidenced by the partial water solubility of the products.

Most preparations in which HCl was a reactant were unsatisfactory due to incomplete chlorination which resulted either from equipment

Table I: Analytical Results

Compound	wt% Chlorine		wt% Ytterbium	
	% Observed % C	alculated	% Observed	% Calculated
YbC1 ₂	28.9±0.2ª	29.0	71.0±0.1ª	71.0
YbC1 _{2.26}		YbC1 _{2.26±0.05} b		
		YbC1 _{2.30±0.05} b		
		YbC1 _{2.28±0.05} b		
YbC1 ₃	37.9±0.3 ^c	38.1	62.0±0.2 ^c	61.9
УЬОС1	15.6±0.3 ^c	15.8	77.2±0.2 ^c	77.2

a = error is standard deviation

Table II: Lattice Parameters

Phase	Symmetry	Lattice Constants (Å or deg)	Structure Type	Space Group
YbC1 ₃ ·6H ₂ С) monoclinic	a = $9.60_7 \pm 0.01_4$ b = 6.524 ± 0.008 c = 7.842 ± 0.007 β = $94.18_5 \pm 0.06_3$	GdC1 ₃ ·6H ₂ O	P2/n
У ЬС1 ₃	monoclinic	a = 6.741 ± 0.009 b = 11.657 ± 0.017 c = 6.384 ± 0.008 β = 110.17 ± 0.058	AlCl ₃	C2/m
YbC1 ₂	orthorhombic	a = 6.693±0.001 b = 13.150±0.003 c = 6.943±0.001	CeSI	Pbca
Yb0C1	hexagonal	$a = 3.72_6 \pm 0.001_8$ $c = 55.60_6 \pm 0.008_3$	Yb0C1	
TmOC1	hexagonal	a = 3.732±0.002 c = 55.78±0.11	Yb0C1	
Lu0C1	hexagonal	$a = 3.717 \pm 0.002$ $c = 55.3_7 \pm 0.14$	Yb0C1	

b = estimated error for individual determinations of three samples

c = estimated error for single determination

malfunction or melting of the $YbCl_3$ initially formed. Melting of $YbCl_3$ caused Yb_2O_3 or YbOCl to be occluded and thereby restricted further chlorination.

The NH₄Cl method for preparation of YbCl₃ proved to be the most satisfactory. The product obtained in this manner was a fine white powder which was rapidly and completely water soluble. The extremely hygroscopic samples were stored over P_2O_5 in an evacuated desiccator for periods of less than a week before use.

3. Intermediate Ytterbium Chloride (YbCl_{2,26})

In the course of early attempts to produce YbCl₂ by reduction of YbCl₃, an unreported phase was observed by X-ray analysis. Elemental analyses indicated the composition of the phase was intermediate between those of the di- and trichlorides. Analytical results for several preparations indicated a Cl/Yb ratio which varied from 2.26 to 2.30. X-Ray powder diffraction records are inconclusive as to phase purity because of possible coincidences of diffraction lines with those of YbCl₃ and YbCl₂. The observed interplanar d-spacings are listed in Appendix III-B. The light green phase disolved in water to yield a similarly colored solution which turned rapidly colorless upon addition of dilute HNO₃ - this observation is consistent with the presence of ytterbous ion in solution. Hereafter in this work, the phase will be referred to as YbCl_{2.26} although its exact composition is uncertain.

4. Ytterbium Dichloride

All four methods described for the reduction of YbCl₃ yielded YbCl₂.

To assure complete reduction to the dichloride, prolonged heating (2 hours) at temperatures above 700° was necessary in the thermal and hydrothermic syntheses. Direct synthesis of YbCl₂ from the elements was not attempted.

The bulk of the YbCl₂ used in this investigation was prepared by in <u>situ</u> hydrogen reduction of YbCl₃ as described in (IV-B-3-b). When viewed with reflected daylight, YbCl₂ is colored jade green; samples are light green when viewed with transmitted incadescent light. The interplanar d-spacings for YbCl₂ are listed in Appendix III-C.

Ytterbium dichloride is not nearly as hygroscopic as YbCl $_3$ with several days being needed for a sample of YbCl $_2$ a few milimeters thick to hydrolyze completely in air to the hydrous oxide. Powdered samples hydrolyze rapidly. Dissolution of YbCl $_2$ in water also takes place much more slowly than that of YbCl $_3$. Dilute aqueous solutions of YbCl $_2$ ($\simeq 10^{-3} \text{M}$) remain light green for several hours at room temperature if undisturbed.

5. Ytterbium Oxidechloride

Thermal decomposition of YbCl $_3$ ·6H $_2$ O yielded a product which on the basis of X-ray powder diffraction analysis contained a major component which gave broad bands on the diffraction photographs and a small amount of Yb $_2$ O $_3$. The heating of equimolar amounts of YbCl $_3$ and Yb $_2$ O $_3$ under an inert atmosphere produced similar results. At the upper temperature range of preparations only Yb $_2$ O $_3$ was present in the product remaining in the reaction boat since the chloride was swept from the hot zone by the inert gas.

All preparations in which a chlorine atmosphere was used yielded YbOCl. The sharpness of powder patterns improved with extended heating at temperatures above 800° under a chlorine atmosphere, with diffraction lines gradually replacing the broad bands observed previously.

Annealing times varied from two days at 800° to a few hours at 1100°.

Ytterbium oxidechloride is a white, water-insoluble, air-stable solid

which is pulverized easily. Interplanar d-spacings of the YbOCl powder pattern and their indexing based upon symmetry and cell parameter information obtained from examination of single crystals of YbOCl are presented in Appendix III-D.

6. Other Oxidechlorides

The attempted preparation of Yb₃O₄Cl in a chlorine atmosphere produced a new phase of unknown stoichiometry. The diffraction record is reported in Appendix III-E.

The oxidechlorides of thulium and lutetium prepared by the thermal decomposition of the respective hydrated trichlorides under a chlorine atmosphere are isostructural with YbOCl. Mixed metal oxidechlorides prepared from mixtures of dysprosia or holmia and ytterbia crystallized in two structures - the PbFCl-type when the effective metal radius, as determined below, was equal to or larger than the Ho⁺³ radius, and the YbOCl-type when the effective metal radius was smaller than the Er⁺³ radius. Those samples with an effective metal radius of Er⁺³ are dimorphic as is ErOCl. Effective metal radii were determined according to equation (V-1) from Templeton and Dauben's¹¹⁶ set of trivalent lanthanide crystal radii and the mole fractions, x and (1-x), of the sesquioxides used. Exact limits of cationic radius for each structural type were not established.

$$r_{eff} = xr_{Ln_1} + (1 - x)r_{Ln_2}$$
 (V-1)

B. Structural

1. Unit-Cell Determination

a. Optical Properties

Crystals of YbCl₂ were obtained by fracturing a melt and exhibited no regular external morphology. Observation between crossed polarizers indicated YbCl₂ to be biaxial.

Crystals of YbOCl were in the form of extremely thin colorless plates with a micaceous cleavage plane coincident with the plane of the plates. Some of the crystals exhibited the morphology of a thin regular hexagonal prism. Internal interfacial angles for a number of crystals were determined to be 120±1°. Observation of YbOCl crystals between crossed polarizers showed either no variation as the crystal was rotated or extinction in only part of the crystal when it was viewed normal to the plane of the plates. The crystals were too thin to be examined along the plane of the plates.

b. Systematic Absences and Space Group

Preliminary Weissenberg and precession photographs of $YbCl_2$ established orthorhombic symmetry. Reflections were present for the following conditions:

h00, 0k0, 00 ℓ only when h, k, ℓ = 2n, respectively hk0, 0k ℓ , h0 ℓ only when h, k, ℓ = 2n, respectively hk ℓ no regular extinctions

These conditions are uniquely consistent with space group P $2_1/b$ $2_1/c$ $2_1/a$ (No. 61)⁹⁵ which will be referred to as Pbca. The conditions governing possible reflections and the coordinates of equivalent positions for the general and special position sets of Pbca are found

		;
		•
		i
		;
		i

in Table III. Schematics of the symmetry of the space group are illustrated in Figure 5.

It has not been possible to assign unequivocally a space group for YbOC1. Precession and Weissenberg photographs confirm hexagonal or pseudo-hexagonal symmetry. Systematic absences exist only for 00l = 3n. However, rotation photographs of a second crystal reveal that the translational period of the c*-axis is one-half the period as determined from Weissenberg photographs taken with a* as a rotation axis. Thus the requirement limiting possible reflections is 00l = 6n. This requirement is satisfied for four space groups, $P6_1$ and $P6_122$ and the enantimorph of each, $P6_5$ and $P6_522$. It appears also that hkl reflections for l = 2n are much stronger than those for l = 2n + 1.

c. Lattice Parameters

Refined lattice parameters for YbCl₂ as listed in Table II were determined from least squares fit diffractometer data for (hkl) and $(\overline{h}\overline{k}\overline{l})$ reflections taken as described previously. No angular dependent weighting or extrapolation function was used for the fit.

Refined lattice parameters for YbOCl were obtained from a linear regression fit^{145} of powder diffraction data using the symmetry and approximate lattice periods obtained from single crystal photographs.

d. Density

The density of YbCl₂ derived by the buoyancy method is 5.17±0.05 g cm⁻³ at 23° (the error is estimated). Based upon the observed lattice parameters, this density corresponds to 7.8 molecules per unit cell.

The theoretical density for eight molecules per unit cell is 5.34 g cm⁻³. The density observed by Klemm and Schüth³ at 25° was 5.08 g cm⁻³.

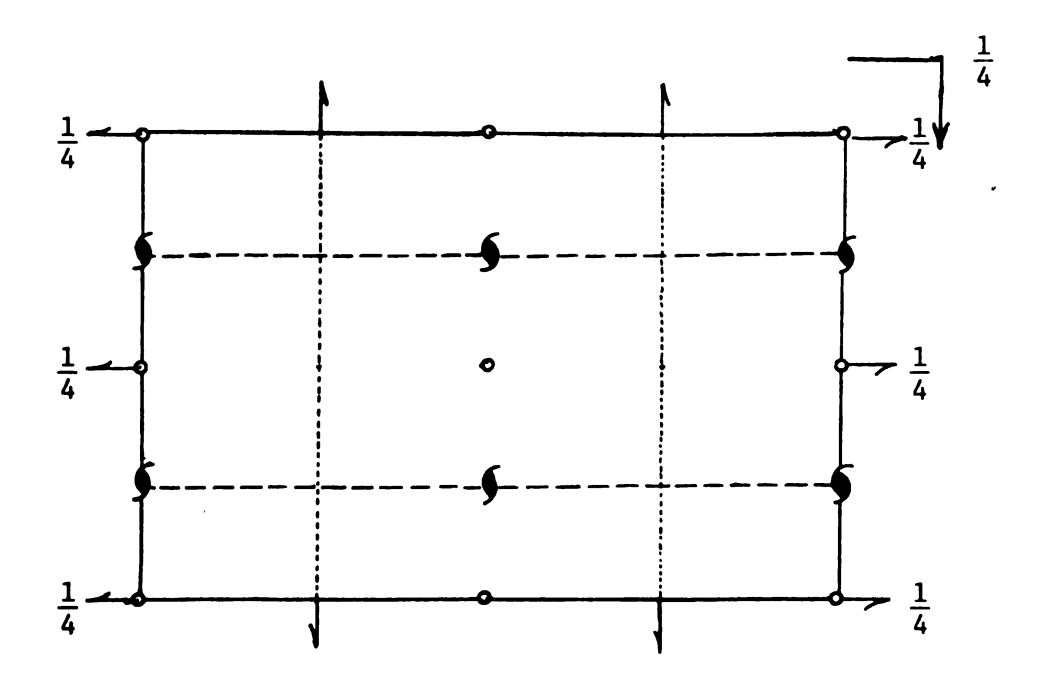
The density of YbOCl was not determined.

			(
			í
			í
			(
			Ś

TABLE III: Properties of Space Group Pbca

Positions	Point Symmetry	Coordinates of Equivalent Positions		nditions for n-extinction									
8c	1	±(x,y,z; 1/2+x,1/2-y,z; x,1/2+y,1/2-z; 1/2-x,y,1/2	+z)	hkl: Okl hOl hkO	No conditions k = 2n l = 2n h = 2n								
4b	ī	0,0,1/2;1/2,1/2,1/2;0,1/2,0;		-	al: as above,								
4a	ī	0,0,0;1/2,1/2,0;0,1/2,1/2; 1/2,0,1/2		plus h+k,	$k+\ell$, $\ell+h=2n$								

FIGURE 5. Representation of Space Group Pbca



		ξ.
		;
		í
		;
		÷
		Ç

2. Intensity Data

a. Data Collection

An approximately right parallelepiped crystal with approximate dimensions of 0.24 x 0.21 x 0.19 mm was mounted and centered on the Eulerian cradle. The ϕ -axis was nearly normal to the (515) plane. Intensities of 495 independent reflections ($\sin \theta/\lambda \le 0.62$) were measured at a 5°30' take-off angle. Intensities of 184 reflections which were not absent because of symmetry were recorded as zero. The ratio of intensities observed was 14084:1. No background correction was made since with the monochromator in place and adjusted for strictly Kal radiation no X-ray background was detected. With the monochromator the intensity of the unfiltered beam was decreased by 80 to 85%. Mosaity of the crystal was not checked.

More than 40 crystals of YbOCl were examined for suitability for intensity data collection. None was found suitable but all exhibited two properties to a varying degree. The first property was twinning along the c-axis as evidenced by a doubling of spots. The second was that for $\ell \neq 6n$ the spots were neither sharp nor distinct. In addition for the $\ell \neq 6n$ case the spots were either badly streaked or on a few occasions absent altogether with only a slight darkening along festoon lines on the Weissenberg photographs.

b. Absorption Correction

The linear absorption coefficient, μ , for YbCl₂ is 945 cm⁻¹. Calculated absorption correction factors varied from 32.3 to 1. For these calculations the crystal was described by six faces with a number of less prominent faces not being included.

3. Computations

Computations were performed on a CDC 3600 or CDC 6500 computer. The programs used for intensity data reduction (INCOR), Fourier functions, and distance and angle calculations (DISTAN) have been described previously 143,117. The program used for absorption calculations (ORABS2) was written by Busing and Levy 118. Atomic scattering factors were taken from values compiled by Cromer and Waber 119 and corrected for anomalous dispersion 105.

4. Patterson Synthesis and Ytterbium Atom Positions

A three dimensional Patterson function was calculated from intensity data which had been corrected for Lorentz, polarization, and monochromator effects, but not absorption. The positions, relative peak heights, and assignments of the larger Patterson peaks are given in Table IV. The assignment of the Patterson vectors for the metals is described below while the other assignments are based on a posteriori observations.

According to the notation of Table III, the possible ytterbium atom positions include: 8 Yb in Wycoff set 8c or 4 Yb in set 4b and 4 Yb in set 4a. Use of sets 4a and 4b was incompatible with the Patterson synthesis results. Also, the lack of many strong face-centered reflections ((hkl) all even or all odd) made it unlikely that the metals were in the face-centered positions 4a and 4b. The Yb atoms were located from Harker planes which for Pbca are: $\pm (1/2+2x,1/2,0)$, $\pm (0,1/2+2y,1/2)$, and $\pm (1/2,0,1/2+2z)$. By examining particular sections of the Patterson, namely peaks two, three, and four in Table IV, values for x, y, and z can be determined. Peak 1 at the origin contains no information about atomic positions. Initial values for the Yb atom were

		3	
			•
			•
		· ·	•
		.5	•

TABLE IV: Positions and Heights of Principal Patterson Peaks

				Relative		
No.	x	У	z	Height	A	ssignment
1	0.00	0.00	0.00	999	origin	
2	0.00	0.50	0.00	679	Yb-Yb	$(1/2\pm2x,1/2,0)$
3	0.50	0.00	0.42	416	Yb-Yb	$(1/2\pm2x,1/2,0)$ $(1/2,0,1/2\pm2z)$
4	0.00	0.27	0.50	387	Yb-Yb	$(0,1/2\pm2y,1/2)$
	0.50	0.50	0.42	281	Yb-Yb*	(U,1/2-2y,1/2)
5 6	0.50	0.28	0.10	172	10-10"	
7	0.06	0.23	0.50	142		
8	0.46	0.23	0.08	92		
9	0.26	0.43	0.30	88	Yb-C1	
10	0.26	0.08	0.30	78	Yb-C1	
11	0.00	0.08	0.50	75 75	ID-CI	
12	0.00	0.07	0.20	75 70	Yb-C1	
13		0.15		68	10-01	
	0.50		0.50		VL 01	
14 15	0.24	0.35	0.20 0.20	62 52	Yb-C1	
16	0.26 0.50	0.00 0.50	0.20	53 51		
17	0.00	0.41	0.10	50		
18	0.18	0.00	0.00	50		
19	0.00	0.43	0.50	48		
20	0.50	0.09	0.50	48		
21	0.50	0.14	0.00	45		
22	0.44	0.32	0.42	44		
23	0.20	0.50	0.00	44		
24	0.00	0.08	0.12	43		
25	0.22	0.31	0.50	42		
26	0.36	0.17	0.38	41		
27	0.00	0.14	0.38	40		
28	0.00	0.36	0.38	40		
29	0.24	0.19	0.50	37		
30	0.26	0.50	0.20	37		

^{*} Peak overlap from adjacent octant

			;
			;

8c (x, y, z) = (0.25, 0.135, 0.04).

5. Solution of the Chlorine Atom Positions

A least-squares refinement which used the phases determined from the Patterson Yb position and the observed structure factor amplitudes refined to an R of 0.36. A difference Fourier synthesis (V-2) calculated from the refined Yb atom position, (0.23, 0.12, 0.04), with an isotropic

$$\frac{1}{v} \sum_{h} \sum_{k} \sum_{\ell} (|F_0| - |F_{\ell}|) \exp[-2\pi i (hx + ky + \ell z)] e^{i\alpha}$$
 (v-2)

thermal parameter had a peak at (0.01, 0.45, 0.25) which was assigned to a Cl atom in set 8c. Three additional cycles of least-squares refinement for the two atoms with isotropic thermal parameters yielded R = 0.31. The position of the other Cl atom at (0.36, 0.21, 0.40) was located in a second difference synthesis. Additional cycles of least-squares refinement reduced the R factor to 0.28.

At this stage during the structural refinement the computations for the absorption effect were completed. With the absorption corrected data and the previously determined positions for the three atoms, three cycles of least-squares refinement with anisotropic thermal parameters yielded R = 0.156. Twelve reflections were deleted from the final calculations because of potential interference from the goniometer head during data collection. The final R value was 0.137. All data were included with unit weighting. Reflections with $F_{\rm O} = 0$ were not included in the calculations.

Final atomic coordinates and with both isotropic and anisotropic thermal parameters with their standard deviations are found in Table V.

The shift in any parameter in the last cycle of refinement was less than 0.1% of its standard deviation. Observed and calculated structure factor amplitudes are given in Table VI. A difference Fourier synthesis indicated

		(
		;
		•
		;
		į.

Table V: Parameters from Least-Squares Refinement.

A. Atomic Coordinates

x	у	Z
0.2293(6)*	0.1121(2)	0.0430(8)
0.355(3)	0.206(2)	0.389(4)
0.503(3)	0.471(1)	0.264(4)
	0.2293(6)*	0.2293(6)* 0.1121(2) 0.355(3) 0.206(2)

B. Thermal Parameters

Atom	β	β ₁₁ β ₁₂	β ₂₂ β ₁₃	β ₃₃ β ₂₃
Yb	2.7(1.2)	2.5(0.2) 0.03(0.15)	0.9(0.2) 0.01(0.20)	4.4(0.2) 0.10(0.14)
C1(1)	2.8(2.3)	2.5(0.9) 1.0(0.7)	1.5(0.7) 0.09(0.7)	6.2(1.5) -0.9(0.8)
C1(2)	1.6(1.8)	1.5(0.7) 0.2(0.6)	2.0(0.6) 0.7(0.6)	2.4(0.9) 0.5(0.9)

^{*}Standard deviations are in parentheses.

		· ·
		;
		,

Table VI: Observed and Calculated Structure Factors.

U		re	•	c	Q 9	C &	. •	9 9	- -	e.	= ;	2 1		9	P #	•	۸.	Ė	<u>.</u>	•		د ه	ġ	<u>.</u>	ě (9 -		Ţ	•	9 9	<u> </u>	<u>-</u>	ςΨ	٩	0												
4	•																																Ş .														
Ě	•		=	r	Ĭ :	7	- 7	370	16	2	•	- P	£	90	8 5														Ē	č !	- =	=	4	2	C												
×	•	- •		-		n e	•	- (0	- (A P			h P.	0	- 0	N -		٠ -	• •	- -	~	٠ د	- (N 6	2 4	-	•	r .	- ^	•	c -		-												
1			•	c	c	c c		_ :		•	R . (A. A		•		•	•	• -	_	-	- (•	•	F (7	, c	C	c	c •		-	۸ ۸	۸,	-												
ن	;	:	0	-17	ě.		£	Ľ ;	8	2	Ē,	9	; :	Ξ	g 0	-	40	9 9	2	ć	î	- 2	Č	0	ê	[2	. 6	2	5	£ 2	Ę.	134	٨	ş :		¥ 6	9	9.		-	0	ž :		30		. ^
Š	:	=		c		- ·	. r	c (, ,	Ľ	<u> </u>			•	; ; ; r	: î	ï	• ;	; ; : :	_	ii c		c	`` \$	۶		ָר פּ	, ,	0	c	, c	2	î '	! c	• •							c	Ç 1	· c s	2	c į	
5		- •		•	i	~ -∙	=	۰.	? 0 -	-	2	ን የ	- . r	•	h :	: X	4	r	• •		•			<u>,</u>	~		<u>.</u>	-	_		-	-	, ,	_	<u> </u>		r	: -				_	<u>.</u> .	<u>-</u>	0	- (, c
¥	•	, 0	•	•	•	0 0	•	0 (2	2	<u> </u>	٤ :	2	2	<u> </u>	2	2	<u>e</u> :	2 5	Ç	٢.	= :	<u> </u>	5	<u>c</u>	2 :	2 9	2 5	2	9	<u> </u>	٢	<u>c</u> :	=	=:	=	= :	==	= :	= =	: =	=	= :	= =	: =	= :	==
1	•	• •	•	•	•			¢ ·	: C	C	C	c ¢	. 4	C		-	-		٠ م	۰,	٠ (٠.	•	•	•	•	~ •	•	•	•	• •		* *	_		-	- 1		۸ (•	•	-	r F	•	•	
24.0	•	9	Ž	\$	ſ	\$	į	9	Ç	9	-263	2	į	6	-	Ş	Š	- 6	۸.	9	9		í	13	č	0	- 6	172	Š	5:	٠ - -		9 5	5	5	۶		6	2:	- 1	ř	1	-		1	-	1 5
8	3	5	•	£	e j		6	2		ě	72	ij	8	ċ	<u>e</u> c	ŗ	Ĕ	F 8	c	ş	5	·	c	£	2	Š	٠ إ		Ę	c ;	- F	5	,	Ę		c	٠ ;	2	0	c r	ť	۲	c	٤ ،	7	c	c c
<u>.</u>	•		-	•	•	c -	· •	•		-	~	n •	r	•	• • -		•	- ·	•	-	~ (-		•	_	R (•		-		n •	0	- :	-	٨,	•	•	c c	-	۸ ۲	•	ď	•	- 6		4	
ı	•									-	C	c •		-			•	• •	•	•	•			•	•	•			•	E (•	•					- ^	~			۰,		,,		,	r •
				Ī												•		•••		•			Ť		•	Ť	•		•			Ī	•														
4	1	}	•	5	۶	<u> </u>	4	-168	127	F.	5	•	Ē	į :	•		22		ç	179	: :	2	•	ď	•	- 5	Î	ï	Ş	٠ -	' =	ξ	Ç (ξ	ζ,	- 1	X ; {	•	4	֓֞֞֞֓֓֓֞֓֓֓֓֓֓֓֓֓֓֓֓֓֓֓֓֓֓֓֓֓֓֓֓֓֓֓֓֓	· 5	4	K :	-	-	*	
8			-					6 6																																						ű.	c o
ر	•		-	•	n i	• •	•	٠,	•	•	•	۱ e	c	- (. ,	•		¢ -	۰ ۸	•	• •		-	٨	•		- ^	•	•		c r	c	- 6	•	• •	•	- •		• 1) c	-	۸ ،	٠,		-	n r.
1		- •		•				۸,	•	,			•	•		•	•	• •						۲.	٠,				_				,,		۸ ۱								•	• •		r	
ų	•	5	Ľ	_	<u>.</u>	2 5	٨	٠,		ŗ	<u>.</u>		-	<u>.</u>	, r.	5	<u>-</u> (• •	¥	•	¥ :		£	€	ç.	• •	٠,	, Ą	o	٠,	- ¢		9 9		\$:		• •	, ,		ŗ. Ģ	. •	ç	•	. 4	; <u>c</u>	Q	9 5
3	7	i	· =	_	= `	·	î	`` T	•	1			-	• ;	.		•		5	_	``	۲,	5	1	1	- 1	ì =	. '	۲		-	•	5		£ 3		2 7	ź	~ ;	-	٠,٢	۶	7		- 1	-	
8	•	-	-	_	•	-		- 9	•	3		. \$, c	C	c (-	•	-	C (€	Ę	=	-	. C		2	6,		ď			۶ ۶		֚֡֞֞֝֓֞֝֓֞֝֟֝֟֝֟֝֟֟֝֓֟֟֝֟֟֓֓֓֓֓֟֟֓֓֓֟֟֓֓֓	-	5	7.		Ē	٠,	•	; ;	•	
۸ ۲	•	•	•	•	•	- ~			•				ď			ľ	C (• •	. 4	ď	r				*		۸ (1 Y	r	"	•			- •		- ·	^ F	•	4	4	4 4 1 0	۳ د	•	
I	•	•	•	ď	c I	٠,	-		-	-		- ^	٠	•	۰,	•	•	۸ ۲	•	r	•	•	•	•	•	• •	•	•		- (¥	* 4	4	٠,	•	٠,	٠ د	c (c c	•	•	C	٠ ،		-	
۲	Ş	7	5	۲	į	2 2	7	<u> </u>	ī	ç	ī i	•	8	7	۲ ۾ د	í	4	٠	8	7	•	9	۶	č	;	9 9	5 5	9	2	ç	- 7	ç	0 4	_	145	•	ē ;	ç	Ç	٠ : :	ě	٤	Ţ.	n e	-	- 1	\$
š	•	· ·	٠.	ş		<u>.</u>	c	5	, c	:	2 :	·	c	= ;	. i			2	•	•	i 6. 9		c	ī	i S	• 9	· ! c	٠ 2	c	- ·		ō	- ·		9 1		ï • •	آ ي:	٠,	ćι į	<u>ر</u> م	آ دِ	c (
٥			-		•	۾ - د	_	<u>-</u> a :	•		· ·	• «	_	-	-		ë c		- -		= :	<u>.</u> • •	•	-	-	•	: :	Ϋ́	•	_ :	; . r	7			1 158	-	; • 1	- 4		5 - 	- 7	-	• (: -		- ~
*	•	•	•	r	•	•	•	•	•	•	r	•	•	F (•	•	•	rr	•	•	•	• •	•	•	•	• •	•	•	•	•	• •	•	• •	•	• •	•	•	•	•	• •	•	•	•	• •	•	•	•
I	•	•	_	•			•	• •		•	- 1	•				ľ	•	.	∢				C	c				-	-	٠ (, ,	•	•	٨	n	٢	•	•	•	• •	•	•	•	• •		• •	7 u
3	3	. 6	1	Ē	= }	7	Ť	8	:	Ë	ě	֓֞֞֝֟֝֓֓֓֓֟֝֟֓֓֓֓֓֓֓֓֓֟	į	5	- 3	7	913	6	7	Î	6		ş	770	2	֓֞֜֜֝֓֓֓֓֓֓֓֓֓֓֓֓֓֓֓֓֡֜֜֜֓֓֓֡֓֓֡֓֜֜֜֓֓֡֓֡֓֡֡֡֡֡֓֡֓֡֡֡֡֡֡	-	1	2	Ç :		ţ	- K	•	£ 3	=	- 6	-	Ŷ	; ;	Ç	7	-	٠,	į	~ (£ ₹
ě	2		6	7.	6		0	۴,	: [<u>c</u>	ž	,	. 14	2	9		c	c c	0	c	4	c c	4	ğ	٠ ;	١		c	c	- 5	8	i	c c	c	c g	c	cc	c	c e	c c	5	4	£ (o c	Ç	c (c p
بر	•		<	4	« (R P	•	r ,		(-	•	ľ	€ ! a	۔ م		•	4 ¥	<	1			•	- 1				c	•	- r		•	r -	•	r -	•	· •		٠,	٠ c	c	-	٠,	r •		¢ i	-
I	Č	: «	c	•	~ ·											•	•	* F F	,	•	•	•	•						~ '			•	r.		r	_				۲ - ۸		•					A P
ی	£	-	2	8	2 9	2	=	<u>.</u>	5	Ę		: :	2	2:	2 2	Ľ	•	V é	2	E.	•	5 9	9	_	<u>.</u>	<u> </u>	£ 5	-	e.	<u>.</u>	9	I	9 9	ξ	ę:	- c	5 9	2 9	5 '	e i		•	9	c :	- ≰	•	۸ ه
3	ï	7	•	Ĭ	T `	1 = r -	•	ž į	*	ě.	-	- i	\		· -		T .	1 ' 	_						ī ' -	•		• 7	=	7'	_	-	•:		*	:	= `	r =	7	• •	•	7	7	- "	: 5	-	٦-
8	•	8	7	5	ē `	- 3	į,	s,		ī	F .			E.	įž	•					-		ž		C (•			127	C (0 0	122	°	200	5		Ë,	7	=	9	- 2	8	-	- (. 6	= '	: с
7	•	ď	0	c	C		C	c	C	c	C (C (. •	C.	- ~	-		r •	-	-	- •		-	r	•			-	•	•		0		. r		•	- : - :	-		r •		_	-	r •	· •	- (
I	•	•	-	-	a (. •	•	• •	•	r	•	c «	•	۲.		-			_	R . (. •		•	e.	a (۸,	•	•	~	F (ne	•	• •	•	• •	•	r ı	r		P C	· e	¢	•	٠.	٠.	۲ ۱	٠,

no major residual peaks present.

C. Thermodynamic

1. X-Ray Fluorescence Calibration

The calibration curves for the Yb $L\alpha_1$ transition were linear over the concentration range of calibration (0.5 - 10 μg Yb). The slope and intercept values with their standard deviations were 782±31 and 110±16 respectively.

2. Neutron Activation Analysis

Results of the NAA experiment were unsatisfactory. The scatter of the data was so large that the precision of the experiment was unacceptible for the current application.

3. Condensation Coefficient

No Yb was detected on the back of the annular target while approximately 49 μ g of Yb were collected on the second target. If the limits of detection of Yb are estimated to be 0.2 μ g it may be concluded that the condensation coefficient for YbCl₂ on cooled aluminum targets is nearly unity. Measured data have therefore not been corrected.

4. Temperature Measurement

Sample and optical cavity temperatures were compared while the system was at typical operating conditions by replacing the target magazine with an optical window and then alternately measuring the temperature of each cavity. Since in the temperature range for which data were collected the sample cavity was three to eight degrees hotter than the optical cavity, the observed temperatures were increased by five degrees to correct for the gradient.

5. Orifice Closure

Numerous experiments failed entirely or were terminated before the full complement of targets had been exposed due to plugging of the orifice with YbCl₂. Closure continued to be a problem even when the tantalum washer was used and the upper surface of the crucible lid was visually observed to be hotter than the rest of the crucible. All data points for a vaporization were rejected if there was evidence of orifice closure. Microscopic examination of crucible lids showed no evidence of creep of YbCl₂ along the top surface of the lid.

6. Vaporization Mode

On the basis of the observations which follow $YbCl_2$ vaporizes congruently with molecular $YbCl_2$ as the vapor species, while YbOCl vaporizes incongruently with the vapor species being $YbCl_2$ or $YbCl_3$ or a mixture thereof. The vaporization modes are represented by equations (V-3)

$$YbCl2(l) = YbCl2(g) (V-3)$$

and (V-4).

$$3YbOC1(s) = Yb_2O_3(s) + (YbC1_2(g) + C1(g))$$
 (V-4)

a. Weight Loss

Total vaporization of YbCl₂ from a graphite crucible yielded 100.4% of the theoretical weight loss for equation (V-3). Weight loss measurements for YbOCl which was vaporized from a thoria-lined graphite crucible yielded 98.7% of the theoretical value of 41.4% loss expected for the reaction proceeding according to equation (V-4).

b. Mass Spectrometer

During the vaporization of $YbCl_2$ only masses attributable to $YbCl_2^+$, $YbCl_1^+$, Yb^+ and Cl_1^+ were observed. At 30 ev the intensity ratios of

YbCl₂⁺:YbCl⁺:Yb were 15:6:1. The appearance potential curves illustrated in Figure 6 indicate that the Yb⁺ observed is from electron impact bond rupture and is not a primary species. The appearance potential of Yb⁺ parent is 6.25ev¹²⁰. Vaporization of YbOCl as observed with the mass spectrometer took place in two stages. At low temperatures (~400°) only Cl⁺ was observed, while at higher temperatures (>700°) YbCl₂⁺ and its fragments were observed.

c. Effusate Collection

The effusate collected from over the $YbCl_2$ vaporization was determined by X-ray powder diffraction analysis to be $YbCl_2$.

d. X-Ray Examination

X-Ray examination of residues from YbCl $_2$ vaporizations indicated the presence of only YbCl $_2$. Residues from YbOCl vaporizations contained Yb $_2$ 0 $_3$ and YbCl $_2$, or only Yb $_2$ 0 $_3$.

7. Vapor Pressure Equation

Temperature and corresponding equilibrium vapor pressure values determined for reaction (V-3) are presented in Appendix IV and Figure 7. The pressure equation for 49 independent measurements for gaseous YbCl₂ in equilibrium with liquid YbCl₂ together with the standard deviations for the least-squares fit is:

$$\log P_{\text{YbCl}_2}(\text{atm}) = -(1.12_7^{\pm 0.02}_5) \times \frac{10^4}{T} + 4.65^{\pm 0.2}_0$$
 (V-5)

for $1048 \le T \le 1483$ °K.

8. Thermodynamic Values Employed in Data Reduction

Values for $(H_T^{\circ} - H_{298}^{\circ})$ and $(S_T^{\circ} - S_{298}^{\circ})$ for $YbCl_2(s)$ were obtained by graphical interpolation of estimates^{30,31}. Heat capacity, enthalpy, and entropy data are not available for gaseous $YbCl_2$. Brewer et al. 121 reported that available electron diffraction data for the dihalides of

FIGURE 6. Appearance Potential Curves.

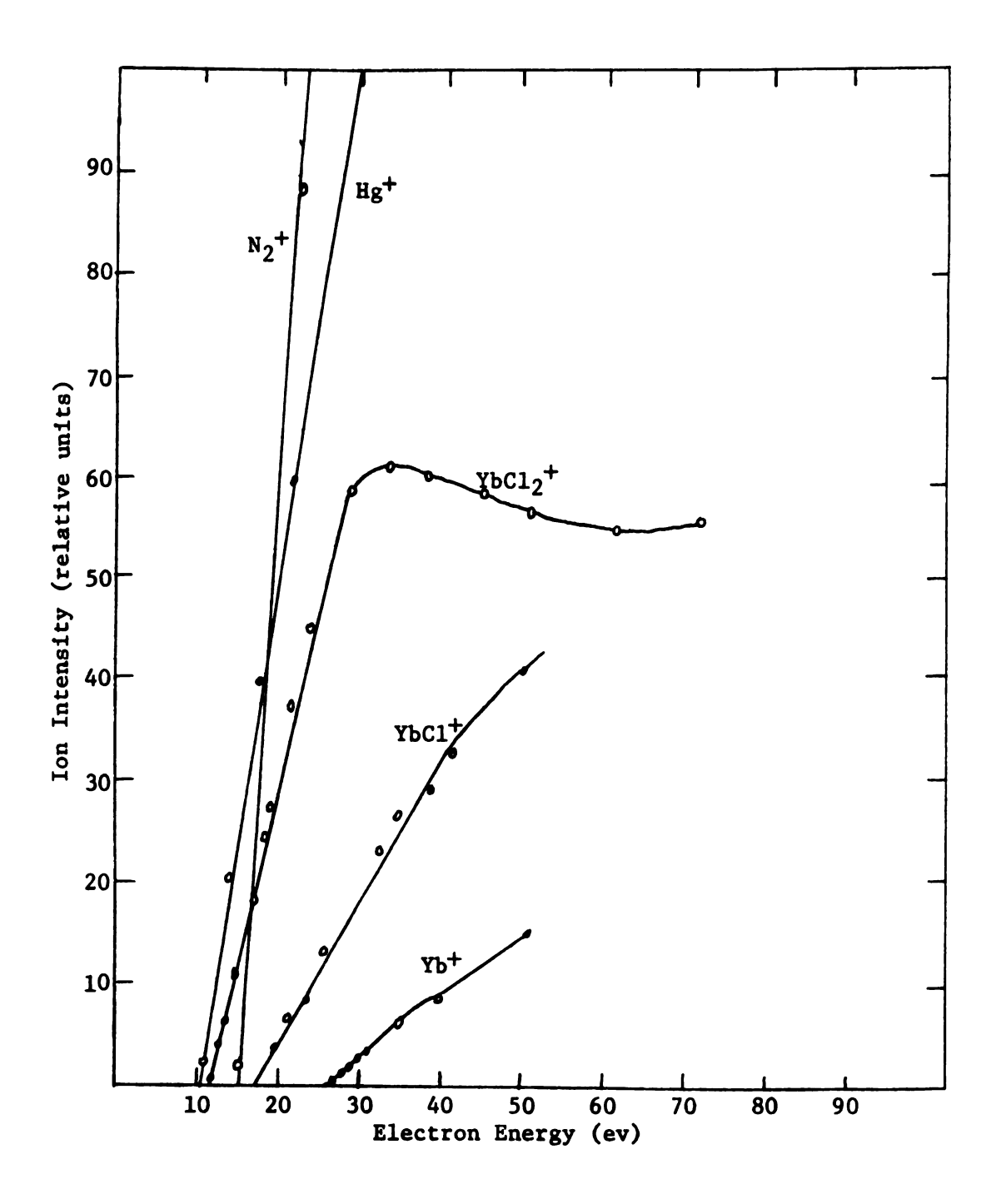
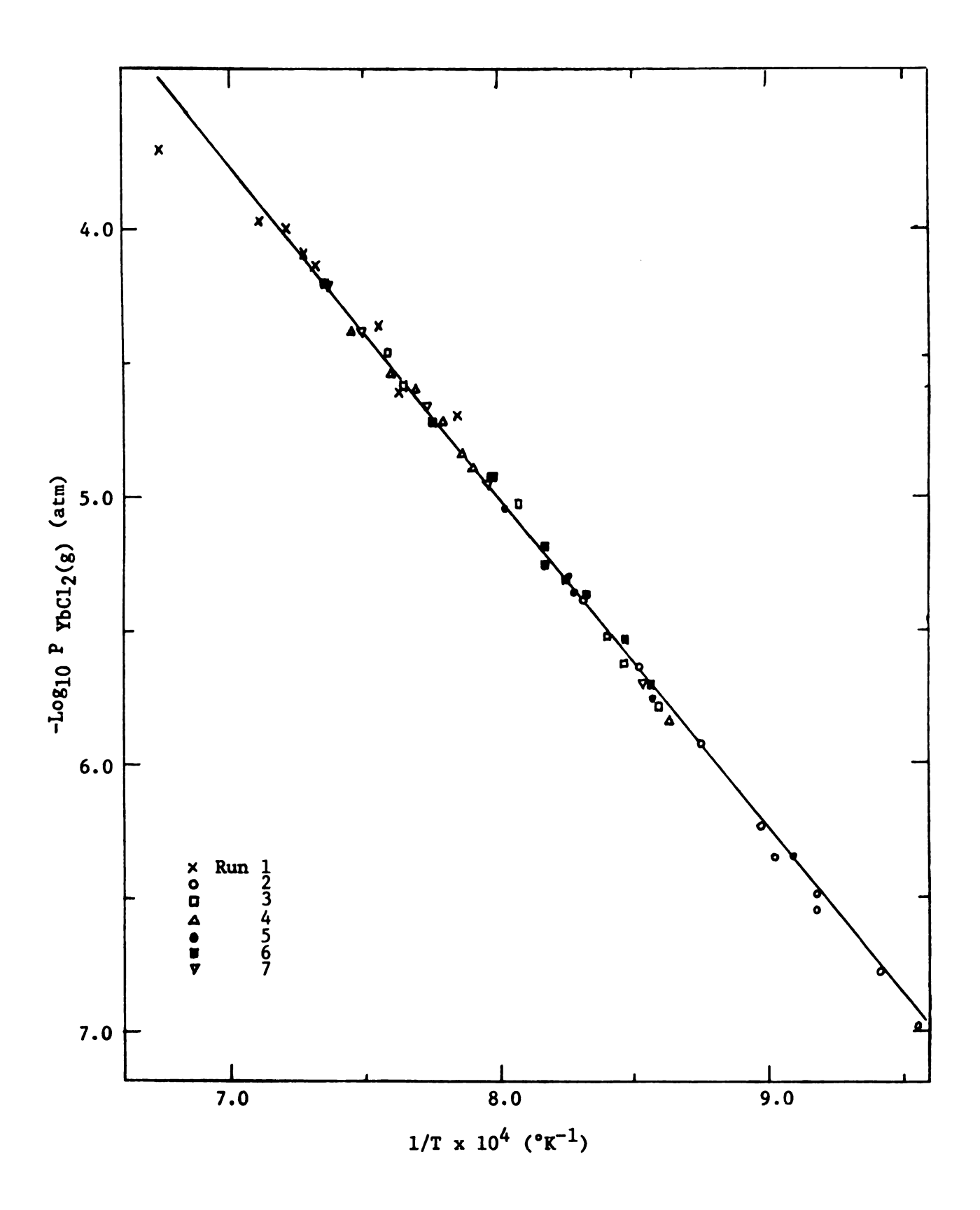


FIGURE 7. Pressure of $YbCl_2(g)$ in Equilibrium with $YbCl_2(l)$.



the alkaline earth and zinc group metals indicate that they possess a linear structure $(D_{\infty}h)$. Since the ground and first excited states of the divalent zinc group metals and Yb⁺² have the same term symbols and all have a d^{10} or $d^{10}f^{14}$ configuration it is reasonable to assume that YbCl₂(g) is also linear. Therefore the experimental data for gaseous mercuric dichloride¹²² were selected for YbCl₂(g) and then corrected for the molecular weight difference by the Sackur relationship¹²³. These data are presented in Appendix V.

The absolute entropy of $YbCl_2(s)$ was determined in two ways. First, Westrum's¹²⁴ value for the lattice contribution to entropy for Yb was combined with Latimer's¹²⁵ value for Cl $(S_{298}^{\circ} YbCl_2(s) = 30.7 \text{ eu})$. Second, the experimental¹²⁶ absolute entropy for $CaCl_2(s)$ was combined with the values for Yb and Ca to obtain another estimate of $S_{298}^{\circ} YbCl_2 = 31.0 \text{ eu}$. The entropy for $YbCl_2(g)$ was taken from the $-fef_{298}$ value for the mass corrected $HgCl_2(g)$ data and numerically equals 70.3 eu.

Free energy functions for both condensed and gaseous $YbCl_2$ were calculated from the estimated and experimental data for $HgCl_2$. Heat capacity data for $HgCl_2$ were also employed. Values for Δfef for the vaporization were obtained by graphical interpolation of calculated data.

9. Thermochemical Values

Results of the vaporization of YbCl₂(ℓ) according to equation (V-3) were treated in the following way. From the pressure equation (V-5) (median temperature 1265°K), values of $\Delta H_{1265}^{\circ} = 55.2^{\pm}1.2$ kcal mole⁻¹ and $\Delta S_{1265}^{\circ} = 21.3^{\pm}0.9_4$ eu were obtained, and were reduced to 298°K using approximated heat capacity data. For the sublimation of YbCl₂(s), $\Delta H_{298}^{\circ} = 61.8^{\pm}2.3$ kcal mole⁻¹ and $\Delta S_{298}^{\circ} = 31.1^{\pm}2.0$ eu. The

enthalpy and temperature of fusion of YbCl₂(s) were assumed equal to those for $HgCl_2(s)$. Combination of the measured pressure data and the extrapolated free energy functions according to equation (III-15) yielded a third law $\Delta H_{298}^2 = 59.7_3 \pm 0.8_0$ kcal mole⁻¹ with no temperature dependent trend in the values. These independent third law enthalpy data are presented in Appendix IV.

The energetics of formation were calculated in the following manner. Combination of the enthalpies of formation of $Yb(g)^{127}$ and $Cl(g)^{122}$ and the estimated energy of dissociation of $YbCl_2(g)^{128}$ gave an estimated ΔH_f^2 298 $YbCl_2(g)$ of-119.8 ± 3.6 kcal mole⁻¹. If this value is combined with the second law enthalpy of sublimation, ΔH_f^2 298 $YbCl_2(g)$ = -181.8 ± 3.6 kcal mole⁻¹. The second law absolute entropy of $YbCl_2(g)$ (S_{298}^2 = 31.7 eu) was obtained from the entropy of vaporization and the estimated entropy of $YbCl_2(g)$. From these values the free energy of formation ΔG_f^2 298 $YbCl_2(g)$ = -175.3 kcal mole⁻¹. From the entropy of sublimation and ΔS_{f}^2 298 $YbCl_2(g)$ a value of ΔS_{f}^2 298 $YbCl_2(g)$ = 36.0 ± 2.0 eu was obtained. Combination of this value with the estimated enthalpy of formation gives ΔG_{f}^2 298 $YbCl_2(g)$ = -109.7 kcal mole⁻¹.

The normal boiling point of $YbCl_2(\ell)$ was calculated from vapor pressure equation (V-5) to be 2242°K. The enthalpy of vaporization was estimated from the $HgCl_2(\ell)$ data to be ΔH_V° 2242 $YbCl_2(\ell)$ = 48.8 kcal mole⁻¹. Since at the boiling point, $\Delta S_V^{\circ} = \Delta H_V^{\circ}/T_b$, an entropy of vaporization ΔS_V° 2242 = 20.8 eu was obtained.

CHAPTER VI

DISCUSSION

A. Evaluation of Experimental Conditions

1. Neutron Activation Analysis

Several factors contributed to the lack of success of the NAA experiment. Among these were the unavailability of a multi-channel analyzer which could be used to discriminate the Yb radiation from background and the need to wait more than a week after irradiation before the samples could be transported for counting. Since the integrity of the polyethylene encapsulation was destroyed during irradiation, the possibility that some sample washed off the quartz discs while they were in the water pit of the reactor cannot be discounted. Now that facilities are available at Michigan State for irradiation and counting, NAA experiments should be reconsidered as an external check on the accuracy of the X-ray fluorescence analyses and should verify the gold calibration experiments 77.

2. Fluorescence Analysis

Fluorescence analysis of the collected effusate proved satisfactory. At the 2 μ g level reproducibility is estimated to be \pm 5%. The major disadvantage was the tedium of the counting procedure.

The intercept of the calibration curve deviates from the expected

0.0 position, even though 0.0 was included as a datum point. This deviation probably results because the Ni $K\alpha_2$ transition occurs within 0.1° of the measured Yb transition. Since a 0.5° scan was utilized the Ni transition was always included. Nickel, together with iron and copper, was present as a trace impurity in the aluminum targets. Elimination of the Ni interference by selection of another Yb transition is not practical because of the decreased sensitivity which would result.

The recently acquired vacuum spectrometer and associated counting equipment should allow use of a fixed angle rather than a scanning procedure and should result in a reduction of the time necessary for analysis. A second advantage of the vacuum spectrometer is that analysis could have been conducted for chlorine as well as ytterbium.

3. Temperature Measurements

The systematic error in temperature measurement due to calibrations of the pyrometers to the 1948 International Temperature Scale is quoted to be ± 4° in the National Bureau of Standards certification. Random errors due to observer error in use of the pyrometer are estimated to be ± 3° as determined from a number of successive readings of the standard lamp's temperature taken within a short period. The crucible cavity observed to measure sample temperature had an orifice area to depth ratio of less than 1:9, a value generally assumed to approach blackbody conditions so that no emissivity correction was made.

4. Orifice Closure

A definitive explanation for the closure of the orifice with YbCl₂ during vaporization has not been found. It is possible that

΄.
;
,
(

some radiative losses immediately adjacent to the orifice area allow condensation of the liquid. Once condensation of a non-conducting substance has occured, rapid orifice plugging would follow. Use of the graphite oven as a susceptor minimized these radiative losses.

5. Knudsen Conditions

Attainment of Knudsen conditions is evidenced by consideration of trends in the experimental data. The regularity of the temperature-pressure data with variation of orifice area and with varying temperature suggests that deviations arising from sampling and non-equilibrium problems are less than the experimental uncertainty.

6. Crucible Materials

Weight loss data and visual examination indicated that graphite was a suitable material for the vaporization of YbCl₂. Use of a thoria lined crucible for decomposition of YbOCl prevented the ytterbia formed from reacting with the graphite.

7. Density Measurement

For greatest sensitivity in making density measurements by the buoyancy technique, the density of the fluid should be as close to the density of the crystal as is practical. Lack of suitable room-temperature fluids with densities of five to seven g cm⁻³ hampers precise density determination of lanthanide compounds.

8. Intensity Data Collection

It was determined after the completion of the collection of the intensity data that alignment of the \$\phi\$-axis of the cradle was not rigidly fixed. Since in the stationary crystal-stationary detector method only peak height data are collected, variation in the \$\phi\$-axis alignment had the same severe effect as missetting the angles. The

φ-axis spindle and bearing surfaces have been remachined in the hope that future alignment of the Eulerian cradle may be maintained rigidly.

A scanning procedure for intensity data collection was not selected because of difficulties encountered in the initial setup of the Eulerian cradle. An $\omega/2\theta$ -scan was not practical due to low count rates and the inability to mechanically obtain repeated scans.

B. Evaluation of Thermochemical Values Obtained

1. Vaporization Mode

It has been confirmed that YbCl₂ vaporizes congruently with molecular YbCl₂ as the only gaseous species. Gilles⁸¹ lists the stability of the gaseous phase as being a predominating factor in fixing the vaporization mode. In view of the observation of YbCl₂ in the residue of YbOCl decompositions which were conducted below 700°, it is concluded that the relative stabilities of YbCl₂ and YbCl₃ will be an overriding factor in establishing vaporization modes of phases in the Yb-O-Cl system. The stability of Yb₂O₃ is the determining factor for the oxygen-rich portion of the system.

2. Thermodynamic Approximations

Other than second-third law enthalpy agreement which serves as a check on the constancy of heat capacity and entropy approximations, little evidence for their accuracy exists. The data do form a consistent set.

The error introduced into the data reduction by use of the enthalpy of fusion of HgCl_2 ($\Delta\mathrm{H}_\mathrm{m}^\circ$ = 4.15 kcal mole⁻¹) is estimated to be \pm 1 kcal mole⁻¹. The estimate is based upon a comparison of the enthalpy of fusion of CaCl_2 ($\Delta\mathrm{H}_\mathrm{m}^\circ$ = 6.78 kcal mole⁻¹) with that

		;
		:
		Ç
		;

of HgCl_2 on the assumption that $\mathrm{YbCl}_2(s)$ will closely approximate $\mathrm{CaCl}_2(s)$. Justification of this assumption lies in the similarities of ionic sizes and crystal structures.

3. Ytterbium Dichloride Data

The value, $\Delta H_{\rm f}^{\circ}$ 298 = -181.8 kcal mole⁻¹, is in agreement with values of -186 kcal mole⁻¹ obtained by Polyachenok and Novikov³⁴ and -184.5 kcal mole⁻¹ obtained by Machlan et al.³⁵. The entropy of vaporization at the boiling point, 2242°K, of 20.8 eu is in good agreement with Trouton's rule and may be compared with the value of 23.4 eu obtained previously³³. The value of the enthalpy of vaporization at the boiling point, 46.8 kcal mole⁻¹, may be compared with the value of 55.7 kcal mole⁻¹ obtained at T_b = 2105°K reported by Polyachenok and Novikov³³. The reason for this apparent discrepancy is difficult to explain since neither the values employed by Polyachenok and Novikov³³ for reduction of their pressure-temperature data taken in the range \simeq 1500 to 1700°K nor the details of their experiment were given.

The higher enthalpy of vaporization observed for their boiling point experiment may be indicative of a vaporization coefficient (α) for YbCl₂(g) from the liquid that is much less than unity. Loehman et al. 129 have shown that in a Langmuir experiment the vaporization coefficients for SrCl₂, CaF₂, and BaF₂ for the monomeric MX₂(g) species are less than unity (0.1 < α < 0.5). However a vaporization coefficient of this magnitude would reduce the discrepancy only by an estimated three to five kcal mole⁻¹. Experimental thermochemical values are listed in Table VII.

C. Structure of Ytterbium Dichloride

The atomic packing in the YbCl₂ structure is pictured in Figure 8. That it crystallizes in the recently reported^{130,131} CeSI-type structure is very reasonable when consideration is given to the radius-ratios derived from Pauling's crystal radii¹³² and the axial ratios which are listed in Table VIII. The two chlorine atoms are chemically as well as crystallographically non-equivalent as can be seen from their environments (Figure 9). The Yb coordination is hard to define. Each Yb atom has chlorine atoms at 2.78, 2.82, 2.85, 3.24, 3.31, 3.39, 3.66, and 4.07 Å. Several of the Cl-Cl separations are shorter than the sum of the atomic radii. A situation similar to this is observed in crystals of PbCl₂¹³³ - the structural type of NdCl₂, SmCl₂, and EuCl₂¹. A short Cl-Cl distance is also observed in the PbFCl-type lanthanide oxidechlorides⁴³.

From Pauling's¹³² crystal radius of 1.81Å for C1⁻ the chlorine atoms are computed to occupy 71% of the cell volume as compared with a 76% packing factor in cubic closest packing. Attempts to determine a Madelung constant for YbC1₂ to be used in a Born-Haber cycle calculation have not yielded a convergent series.

Most MX₂ halides may be categorized into two general structural types¹³³. Those halides in which the cation/anion radius-ratio is large (>0.7) form predominantly ionic structures which generally belong to the fluorite family of structures. Those halides which are moderately ionic crystallize in lattices which are related to the CdI₂-type in which the large anions are arranged in sheets or chains which often approximate spherical close packing with the smaller cations residing in the tetrahedral or octahedral voids. For YbCl₂, the Yb atoms are

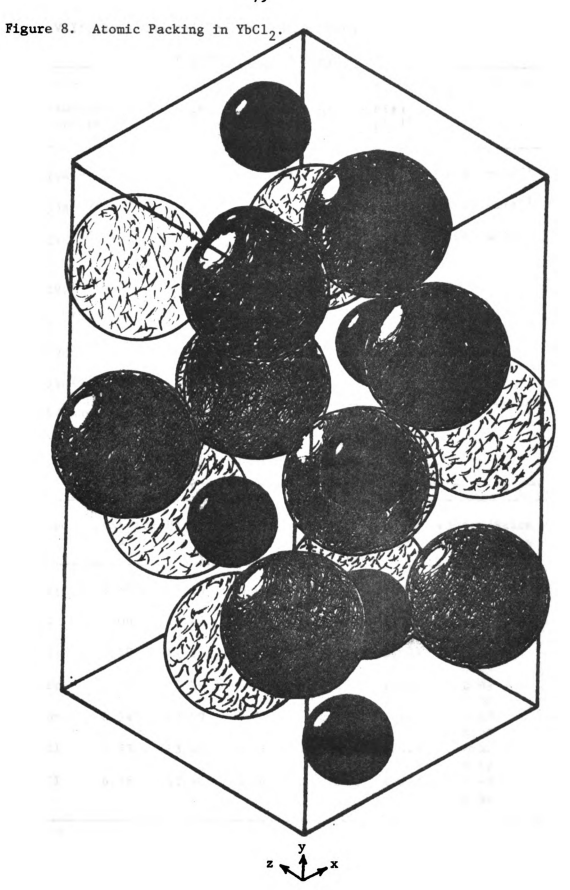


Table VII: Experimental Thermochemical Data.

Ytterbium(II) Chloride

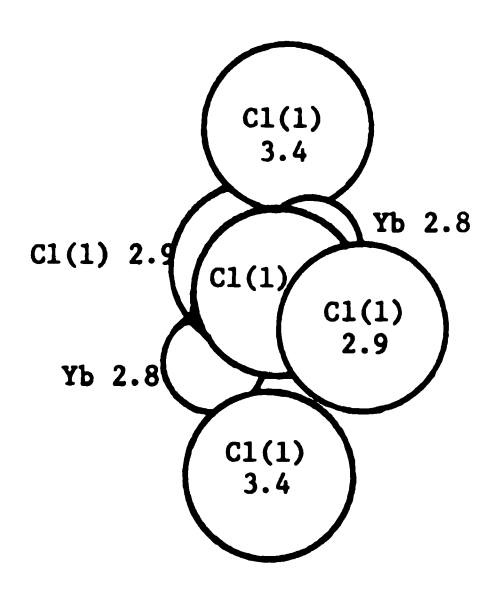
Thermodynamic Property	This Work	Polyachenok Novikov ^{33,34}	Machlan et al. 35	
-ΔH _f 298 YbC1 ₂ (s)	181.6	186	184.5	kcal mole-1
-ΔG _f 298 YbCl ₂ (s)	175.3			$kcal mole^{-1}$
ΔH _v 298 YbCl ₂ (s)	61.2 ^a 59.7 ^b			kcal mole-1
$\Delta S_{v}^{\circ} 298 \text{YbCl}_{2}(s)$	31.1			eu
ΔS° bp YbCl ₂ (l)	20.8	23.4		eu
S° 298YbCl ₂ (s)	30.7			eu
S° 298YbCl ₂ (g)	61.8			eu

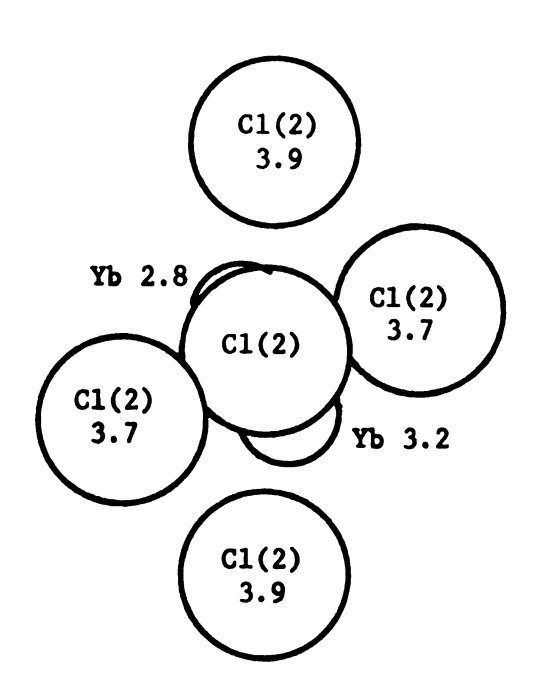
aSecond Law Value; bThird Law Value

Table VIII: Compounds with the CeSI-type Structure.

Compound	Lattice Parameters (A)			Axial Ratios		Cation/Anion
	a	Ъ	С	a/c	b/c	Radius-Ratio
Yьс1 ₂	6.693	13.150	6.942	0.966	1.899	0.58
CeSI	7.06	14.42	7.35	0.960	1.962	0.51 0.61
LaSI	7.10	14.57	7.38	0.962	1.974	0.62 0.53
LaSBr	7.02	13.99	7.19	0.976	1.946	0.62 0.59
CeSBr	6.94	13.69	7.12	0.975	1.941	0.60 0.57
LaSC1	6.83	13.69	7.04	0.970	1.945	0.62 0.62
CeSC1	6.76	13.46	7.00	0.966	1.923	0.60 0.61

FIGURE 9. Chlorine Environment in YbCl₂.





Numbers are distances from the central atom in A.

arranged between the irregular layers of C1 atoms which are parallel to the (101) plane. The difference in electronegativity between Yb(1.1) and C1(3.5) leads to an estimated 76% ionic character¹³² for the Yb-C1 bond which is consistent with the layer-like structure.

Reindexing of the powder diffraction data as reported by Döll and Klemm⁷ for YbCl₂ on the basis of the cell determined in this work yields agreement with the powder diffraction records obtained in this work. The DyCl₂⁷⁸ and TmCl₂⁷⁹ phases should be reexamined to see if the unit cells as reported should be modified to reflect the CeSI-type structure. A combination of bond distance information obtained from the six lanthanide dichlorides may allow a consistent set of Ln⁺² radii to be determined. Rations of Ln⁺²/Ln⁺³ radii could then be determined to complete the divalent set for all lanthanides since the usual lanthanide contraction would be expected.

The division of the lanthanide dichlorides into two structural types is reasonable in view of the fact that the radius-ratios for the PbCl₂ structure lie in the range from 0.61 to 0.69 while those of the CeSI-type range from 0.51 to 0.61. The ratios for NdCl₂, SmCl₂, and EuCl₂ are 0.66, 0.65, and 0.64 respectively while those of DyCl₂, TmCl₂, and YbCl₂ are 0.61, 0.59, and 0.58. The divalent radii for Nd, Sm, Dy, and Tm were estimated from the Ln⁺²/Ln⁺³ radius-ratios for Eu and Yb.

The size of the crystal used for data collection was ten times the optimum thickness 112 of $2/\mu$ where μ is the linear absorption coefficient. The error in the absorption correction due to imprecise description of the crystal is estimated to be as much as ten percent. No regular variation of $(F_0 - F_c)$ was noted, so no extinction correction was applied. Effects of the mechanical shortcomings of the cradle are difficult to

assess. In the final least-squares analysis there are a number of reflections with F_0 = 0 which on the basis of the large values of F_c should have been observed. It may be that the crystal was not in the reflecting position due to variations of the ϕ axis.

D. Structure of Ytterbium Oxidechloride

Initially YbOCl was indexed using a cell with tetragonal symmetry. The precision of data obtained from Guinier photographs showed a systematic error with increasing θ for the values of $(\sin^2\theta_{obs} - \sin^2\theta_{calc})$ which led to rejection of the tetragonal cell. The error was so small so as not to have been observable on Debye-Scherrer photographs.

The cleavage and single crystal information for YbOC1 are consistent with a layer-type structure. Comparisons with CdI₂ and SiC-type structures and specifically Cd(OH)Cl¹³⁴ and Zn(OH)Cl¹³⁵ show that large values of the c-axis for these hexagonal structures are due to variations in stacking of the layers which are each composed of identical atoms. These stacking variations produce changes in the length of the c-axis without producing corresponding changes in the length of the a-axis or stoichiometry. Irregular packing of layers along the c-axis in YbOC1 may account for some of the abnormalities observed in the diffraction records.

I do not expect that the near extinction of some layers is due to order-disorder of oxygen and chlorine atoms within a layer because of the large difference in their sizes. A strict layer structure is also in agreement with the higher degree of covalency expected for YbOCl when compared with YbCl₂. Total extinction of the (hkl) reflections for l odd is not consistent with the observed OOl = 6n extinction.

Since the diffraction photographs seem to indicate that the Yb layers are "well-behaved" as evidenced by the sharpness of the diffraction spots for certain layers, it may be that a solution of the Yb atom positions can be obtained in a sub-cell of the 55 Å cell. Interatomic distances for all MOCl phases of the PbFCl-type were compared with predicted interatomic distances for PbFCl-type TmOCl, YbOCl, and LuOCl. Lattice parameters for TmOCl, YbOCl, and LuOCl were extrapolated from a plot of Ln⁺³ radii versus lattice parameters for the lighter lanthanides. No reason for the structural change in LnOCl which takes place at the Er⁺³ radius was deduced from the interatomic distances.

If the extrapolated value for the density of PbFC1-type YbOC1 is used to calculate the number of molecules in the hexagonal YbOC1 unit cell a value near Z = 12 is obtained. If the possibility of partial occupancy is discounted, then Z = 12 is a reasonable number for the suggested space groups since for these space groups the number of asymmetric units in the cell must be an integral multiple of six. The calculated density for the hexagonal unit cell is 6.7 g cm⁻³, a value some 12% smaller than the extrapolated density of 7.6 g cm⁻³ for the PbFC1-type. This implies that a rather dramatic volume change takes place for the structural change at the Er⁺³ radius. It is difficult to reconcile this apparent discontinuity with a possible bonding scheme for the YbOC1-type structure.

A sample of YbOF prepared by Shinn⁴⁹ was examined in the hope that information which would aid in the solution of the YbOC1 structure would be obtained. X-Ray powder diffraction data indicate that YbOF is dimorphic with d-spacings attributable to both the rhombohedral⁵⁵ and monoclinic⁵⁶ structures present. It is also possible that the sample contained non-stoichiometric YbOF. The only conclusion is that YbOF is not structurally similar to YbOC1.

E. Decomposition of Ytterbium Oxidechloride

Baev and Novikov⁴⁹ report that the estimated free energy change for reaction (VI-1) is zero at 1390° an indication that YbOCl is stable below

$$3YbOC1(s) = YbC1_3(g) + Yb_2O_3(s)$$
 (VI-1)

1390° with respect to disproportionation. However, if an alternate disproportionation reaction (VI-2) is considered the observed lower

$$3YbOC1(s) = YbC1_2(s) + C1(g) + Yb_2O_3(s)$$
 (VI-2)

temperature of decomposition may be rationalized.

Koch and Cunningham¹³⁶⁻¹³⁸ studied the vapor phase hydrolysis of the trichlorides of La, Pr, Nd, Sm, and Gd. They found a linear relationship between the enthalpy of hydrolysis at 785°K and the reciprocal radius of the trivalent lanthanide ion. Their data were replotted using Templeton and Dauben's¹¹⁶ radii and the line extrapolated to obtain for reaction (VI-3) $\Delta H_{785}^{\circ} = 11.8$ kcal mole⁻¹. This value was reduced to

$$YbCl_3(s) + H_2O(g) = YbOCl(s) + 2HCl(g)$$
 (VI-3)

298° K using Koch and Cunningham's 138 free energy function for the samarium system to obtain $\Delta H_{298}^{\circ} = 12$ kcal mole $^{-1}$. Use of published enthalpy data for HCl(g), $H_2O(g)^{122}$ and YbCl₃(s) 30 yielded a value of $\Delta H_{f\ 298}^{\circ}$ YbOCl(s) = -299 kcal mole $^{-1}$.

A value of S_{298}° for YbOC1 was estimated by adding the lattice contributions for each of the ions to obtain 24.1 eu. For this estimate, the contribution of oxygen was taken to be 2 eu; reported estimates of entropies attributable to 0^{-2} range from 0 to 6 eu. Combination of the values of enthalpy and entropy of $Yb_2O_3(s)$ from Westrum¹²³, $YbC1_2(s)$ from this work, and $C1(g)^{122}$ yields a free energy for reaction (VI-2) of $\Delta G_{298}^{\circ} = 43$ kcal mole⁻¹. At higher temperatures, the entropy effect which is largely due to the formation of C1(g) will

become increasingly important and at about 600° K the free energy change for reaction (VI-3) should cross zero. The extremum values for the contribution of 0^{-2} establish a crossover temperature range of $240 \le T \le 1190^\circ$ K (the enthalpy change for the reaction is assumed independent of temperature). This temperature range is consistent with the observations in this work. The strong dependence of the proposed decomposition reaction upon chlorine pressure is in agreement with the ability to prepare YbOC1 crystals at 1100° in the sealed ampoules containing chlorine.

F. On Ytterbium(II) as a Group IIB Ion

In the course of the YbCl₂ study reported herein, I found that references to zinc chemistry were consulted frequently. I propose that consideration needs to be given to classifying Yb with the group IIB elements as well as with the lanthanides. The ground and first two excited states of ytterbium and the zinc group metals are the same. While for Yb⁺² the filled 4d orbitals are lower lying than the 4f orbitals, there are many structural similarities between zinc and ytterbium. In bonding cases where the ionic contribution predominates over the covalent contribution, Yb⁺² often is more like the zinc group metals than the alkaline earth metals. The alloys observed in the ytterbiumzinc phase study¹³⁹ do not support the behavior expected since Hume-Rothery type phases which would be expected for similar metals were not observed. This lack of similarity in the alloy system may result from a size difference.

CHAPTER VII

SUGGESTIONS FOR FUTURE RESEARCH

The number of new questions raised as a result of this investigation is larger than the number of questions answered. However, many of these should be examined so as to develop a unified body of information about the Yb-O-Cl system.

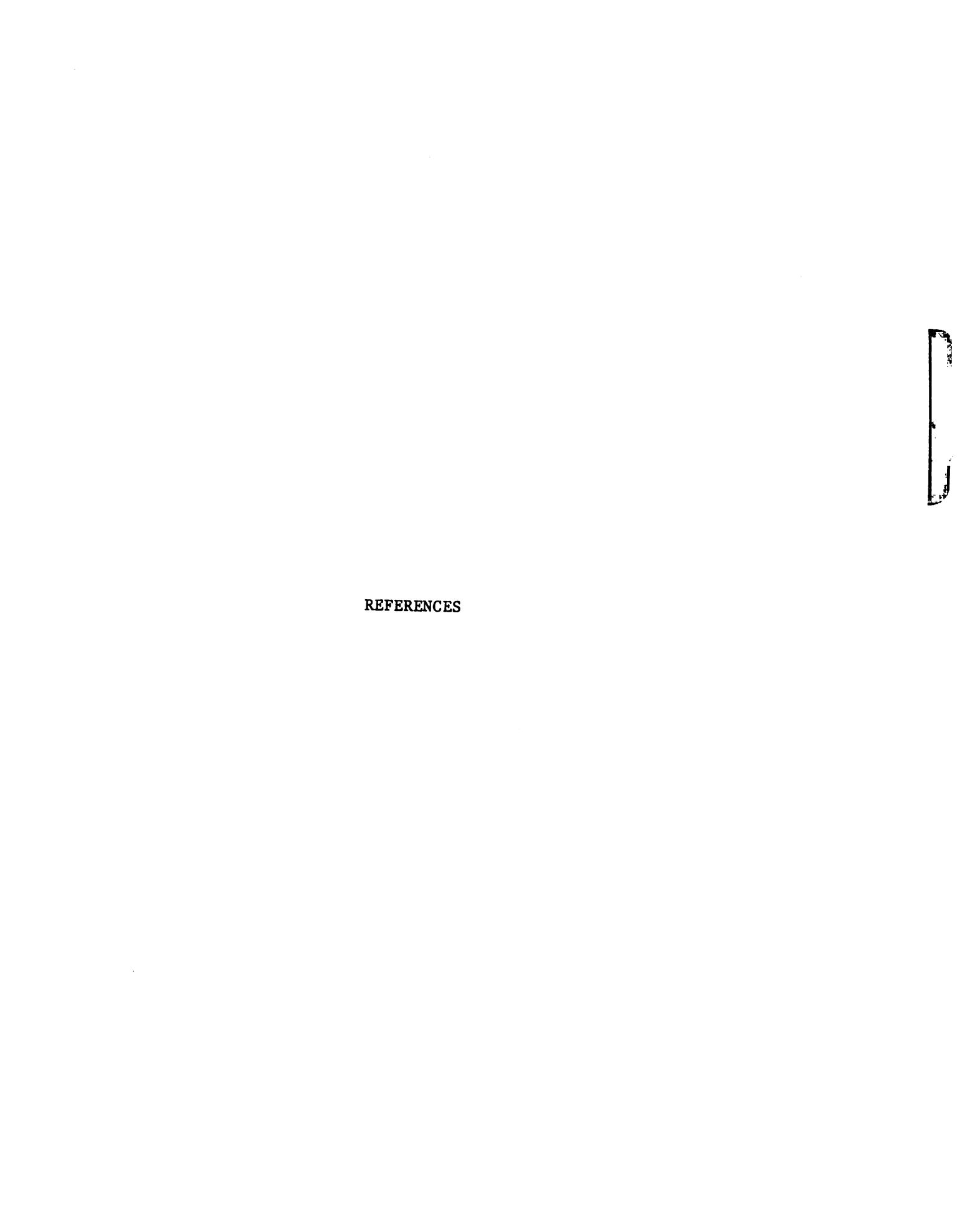
Completion of the YbOCl structure may allow determination of the reason for the structural transition of LnOCl with cationic radius. A change in the conditions of growth for the YbOCl crystals such as by the addition of a small amount of iodine to alter the vapor transport mechanism may produce samples more suitable for a structural study.

A definitive vaporization study of YbCl₃ is necessary to resolve the existing discrepancy as to the vapor species before explicit vapor-ization studies of Yb-O-Cl phases can be completed. The preparative possibilities for the Yb-O-Cl system should bear fruition since only YbOCl has been confirmed and minimal evidence exists for a second ternary phase.

An examination of the Yb-Cl phase diagram in the YbCl₂-YbCl₃ region would be an important step in the testing of Corbett's¹⁴⁰ hypothesis that the sublimation energies of the metals determines the observed stability trend. As has been noted⁷⁷ a system of this type may be amenable to an equilibrium study using spectroscopic determination of equilibrium chlorine pressures.

The structure of stoichiometric YbOF needs to be established as a starting point for a study of the Yb-O-F system of the type in progress¹⁴¹ for Sm-O-F and Eu-O-F.

Experience gained from work with the halides should be used as a basis from which to begin examination of the potentially interesting lanthanide mixed-halide and pseudo-halide systems.



REFERENCES

- D. Brown, "Halides of the Lanthanides and Actinides," John Wiley and Sons Ltd., London 1968.
- 2) W. Klemm and J. Rockstroh, Z. Anorg. Allg. Chem., 176, 181 (1928).
- 3) W. Klemm and W. Schüth, <u>ibid.</u>, 184, 352 (1929).
- 4) G. Jantsch, H. Grubitsch, and H. Alber, <u>ibid.</u>, 185, 49 (1929).
- 5) G. Jantsch, N. Skalla, and H. Jawurek, <u>ibid.</u>, 201, 207 (1931).
- 6) W. Klemm and W. Döll, <u>ibid.</u>, 241, 233 (1939).
- 7) W. Döll and W. Klemm, <u>ibid.</u>, 241, 239 (1939).
- 8) G. Jantsch, H. Alber, and H. Grubitsch, Monatsh. Chem., 53-54, 305 (1929).
- 9) M. Taylor, Chem. Rev., 62, 503 (1962).
- 10) K. E. Johnson and J. R. Mackenzie, <u>J. Inorg. Nucl. Chem.</u>, 32, 43 (1970).
- 11) G. I. Novikov and O. G. Polyachenok, <u>Usp. Khim.</u>, <u>33</u>, 732 (1964); <u>Chem. Rev. USSR</u>, <u>33</u>, <u>342</u> (1964).
- 12) J. K. Howell and L. L. Pytlewski, J. Less-Common Metals, 18, 437 (1969).
- 13) S. Mroczkowski, <u>J. Crystal Growth</u>, 6, 147 (1970).
- 14) D. H. Templeton and G. F. Carter, <u>J. Phys. Chem.</u>, 58, 940 (1954).
- 15) W. W. Wendlandt and J. L. Bear, Anal. Chim. Acta, 21, 439 (1959).
- 16) W. W. Wendlandt, <u>J. Inorg. Nucl. Chem.</u>, 9, 136 (1959).
- 17) G. Haeseler and F. Matthes, J. Less-Common Metals, 9, 133 (1965).
- 18) S. J. Ashcroft and C. T. Mortimer, <u>ibid.</u>, 14, 403 (1968).
- 19) A. Pabst, Amer. J. Sci., 22, 426 (1931).

- 20) M. Marezio, H. A. Plettinger, and W. H. Zachariasen, Acta Crystallogr., 14, 234 (1961).
- 21) N. K. Bel'skii and Yu. T. Struchkov, <u>Soviet. Fiz. Cryst.</u>, 10, 15 (1965).
- 22) E. J. Graeber, G. H. Conrad, and S. F. Duliere, <u>Acta Crystallogr.</u>, 21, 1012 (1966).
- 23) L. F. Druding and J. D. Corbett, <u>J. Amer. Chem. Soc.</u>, 83, 2462 (1961).
- 24) O. G. Polyachenok and G. I. Novikov, <u>Zh. Obsch. Khim.</u>, 33, 2797 (1963); <u>J. Gen. Chem. USSR</u>, 33, 2900 (1963).
- 25) H. Bommer and E. Hohmann, Z. Anorg. Allg. Chem., 248, 373 (1941).
- 26) "Selected Values of Chemical Thermodynamic Properties," National Bureau of Standards Circular 500, U. S. Government Printing Office, Washington, D. C., 1950.
- 27) F. H. Spedding and C. F. Miller, <u>J. Amer. Chem. Soc.</u>, 74, 4195 (1952).
- 28) F. H. Spedding and J. P. Flynn, ibid., 76, 1474 (1954).
- 29) F. H. Spedding and J. P. Flynn, <u>ibid.</u>, 76, 1477 (1954).
- 30) L. Brewer, L. A. Bromley, P. W. Gilles, and N. L. Lofgren, "Chemistry and Metallurgy of Miscellaneous Materials: Thermodynamics," L. L. Quill, Ed., McGraw-Hill Book Co., Inc., New York, NY, 1950, paper 6.
- 31) L. Brewer, <u>ibid.</u>, paper 7.
- 32) O. G. Polyachenok and G. I. Novikov, <u>Zh. Neorg. Khim.</u>, 8, 1567 (1963); <u>J. Inorg. Chem. USSR</u>, 8, 816 (1963).
- 33) O. G. Polyachenok and G. I. Novikov, <u>ibid.</u>, 8, 2631 (1963); <u>ibid.</u>, 8, 1378 (1963).
- 34) O. G. Polyachenok and G. I. Novikov, <u>Vestn. Leningr. Univ., Ser. Fiz. Khim.</u>, 18, 133 (1963); <u>Chem. Abstr.</u>, 60, 4875b (1964).
- 35) G. R. Machlan, C. T. Stubblefield, and L. Eyring, <u>J. Amer. Chem. Soc.</u>, 77, 2975 (1955).
- 36) C. T. Stubblefield and L. Eyring, ibid., 77, 3004 (1955).
- 37) C. T. Stubblefield, Ph. D. Thesis, State University of Iowa, Iowa City, IA, 1954; Diss. Abstr., 15, 1180 (1955).

- 38) D. A. Johnson, <u>J. Chem. Soc.</u>, A, 1969, 2578 (1969).
- 39) J. L. Moriarty, <u>J. Chem. Eng. Data</u>, 8, 422 (1963).
- 40) O. G. Polyachenok and G. I. Novikov, <u>Zh. Neorg. Khim.</u>, 9, 773 (1964); <u>J. Inorg. Chem. USSR</u>, 9, 429 (1964).
- 41) J. M. Stuve, <u>U. S. Bur. Mines</u>, Rep. Invest., No. 6902 (1967).
- 42) G. I. Novikov and A. K. Baev, <u>Izv. Vysshikh. Uchebn. Zavedenii</u>, <u>Khim. Khim. Tekhnol.</u>, 9, 180 (1966); <u>Chem. Abstr.</u>, 65, 9824g (1966).
- 43) D. H. Templeton and C. H. Dauben, <u>J. Amer. Chem. Soc.</u>, 75, 6069 (1953).
- 44) R. I. Slavkina, G. E. Sorokina, and V. V. Serebrennikov, <u>Tr. Tomsk. Gos. Univ., Ser. Khim.</u>, 157, 135 (1960); <u>Chem.</u> <u>Abstr.</u>, 61, 7927h (1964).
- 45) M. M. Bel'kova and L. A. Alekseenko, <u>Zh. Neorg. Khim.</u>, 10, 1374 (1965); <u>J. Inorg. Chem. USSR</u>, 10, 747 (1965).
- 46) I. S. Morozov and B. G. Korshunov, Zh. Neorg. Khim., 1, 2606 (1956).
- 47) I. S. Morozov and B. G. Korshunov, <u>Dokl. Akad. Nauk SSSR</u>, 119 525 (1958).
- 48) A. K. Baev and G. I. Novikov, Zh. Neorg. Khim., 10, 2457 (1965); J. Inorg. Chem. USSR, 10, 1337 (1965).
- 49) D. B. Shinn, Ph. D. Thesis, Michigan State University, East Lansing, MI, 1968.
- 50) K. F. Zmbov and J. L. Margrave, <u>J. Less-Common Metals</u>, 12, 494 (1967).
- 51) K. F. Zmbov and J. L. Margrave, "Mass Spectrometry in Inorganic Chemistry," Advances in Chemistry Series, No. 72, American Chemical Society, Washington, D. C., 1968, pp 267-290.
- 52) L. B. Asprey, F. H. Ellinger, and E. Staritzky in "Rare Earth Research," Vol. II, K. S. Vorres, Ed., Gorden and Breach, New York, NY, 1964, p 11.
- 53) R. G. Bedford and E. Catalano in "8th Rare Earth Research Conference," T. A. Henrie and R. E. Lindstrom, Eds., Reno, NV, Apr. 1970, pp 388-399.
- 54) K. S. Vorres and R. Riviello in "Rare Earth Research IV," Gorden and Breach, New York, NY, 1964, p 521.
- 55) N. V. Podberezskaya, L. R. Batsanova, and L. S. Egorova, Zh. Strukt. Khim., 6, 850 (1965); J. Struct. Chem. USSR, 6, 815 (1965).
- 56) U. Roether, Ph. D. Thesis, Albert Ludwigs University, Freiburg, Breisgau, 1967.

- 57) I. Mayer and S. Zolotov, <u>J. Inorg. Nucl. Chem.</u>, 27, 1905 (1965).
- 58) F. H. Spedding and A. H. Daane, Metallurgical Rev., 5, 297 (1960).
- 59) H. Czeskleba, Michigan State University, personal communication, 1970.
- 60) W. H. Zachariasen, Acta Crystallogr., 2, 388 (1949).
- 61) S. Fried, F. Hagemann, and W. H. Zachariasen, J. Amer. Chem. Soc., 72, 771 (1950).
- 62) I. Mayer, S. Zolotov, and F. Kassierer, <u>Inorg. Chem.</u>, 4, 1637 (1965).
- 63) F. Weiger and V. Scherrer, Radiochim. Acta, 7, 40 (1967).
- 64) N. Schultz and G. Reiter, Naturwissenschaften, 54, 469 (1967).
- 65) H. Bärnighausen, G. Brauer, and N. Schultz, Z. Anorg. Allg. Chem., 338, 250 (1965).
- 66) L. B. Asprey, T. K. Keenan, and F. H. Kruse, <u>Inorg. Chem.</u>, 3, 1137 (1964).
- 67) A. A. Men'kov and L. N. Kommissarova, <u>Zh. Neorg. Khim.</u>, 9, 766, (1964); <u>J. Inorg. Chem. USSR</u>, 9, 425 (1964).
- 68) L. B. Asprey and F. H. Kruse, <u>J. Inorg. Nucl. Chem.</u>, 13, 32 (1960).
- 69) F. H. Kruse, L. B. Asprey, and B. Morosin, Acta Crystallogr., 14, 541 (1961).
- 70) H. Bärnighausen, Agnew. Chem., 75, 1109 (1963).
- 71) H. Bärnighausen, <u>J. Prakt. Chem.</u>, 14, 313 (1961).
- 72) J. W. Hastie, P. Ficalora, and J. L. Margrave, J. Less-Common Metals, 14, 83 (1968).
- 73) S. Natansohn, <u>J. Inorg. Nucl. Chem.</u>, 30, 3123 (1968).
- 74) J. M. Haschke, Arizona State University, personal communication, 1970.
- 75) L. Ya. Markovskii, E. Ya. Pesina, Yu. A. Omel'chenko, and Yu. D. Kondrashev, <u>Zh. Neorg. Khim.</u>, 14, 14 (1969); <u>J. Inorg. Chem. USSR</u>, 14, 7 (1969).
- 76) B. Frit, M. Moakil Chbany, B. Tanguy, and P. Hagenmuller, <u>Bull.</u>
 <u>Soc. Chim. Fr.</u>, 1968, 127 (1968).
- 77) J. M. Haschke, Ph. D. Thesis, Michigan State University, East Lansing, MI, 1969.

- 78) J. D. Corbett and B. C. McCollum, <u>Inorg. Chem.</u>, 5, 938 (1969).
- 79) P. E. Caro and J. D. Corbett, <u>J. Less-Common Metals</u>, 18, 1 (1969).
- 80) J. W. Gibbs, "The Scientific Papers of J. Willard Gibbs," Vol. I, Dover Publishing Ltd., New York, NY, 1961.
- 81) P. W. Gilles, "Vaporization Processes" in "The Characterization of High-Temperature Vapors," J. L. Margrave, Ed., John Wiley and Sons, Inc., New York, NY, 1967, Chapter 2.
- 82) E. D. Cater in "Techniques in Metals Research," Vol. IV, R. A. Rapp, Ed., Wiley-Interscience, Inc., New York, NY, in press.
- 83) M. Knudsen, Ann. Phys., 28, 75 (1909); English Translation by L. Venters, Argonne National Laboratory, Lemont, IL (1958).
- 84) M. Knudsen, ibid., 28, 999 (1909); English Translation by K. D. Carlson and E. D. Cater, Argonne National Laboratory, Lemont, IL (1958).
- 85) K. C. Wang and P. G. Wahlbeck, J. Chem. Phys., 47, 4799 (1967).
- 86) K. C. Wang and P. G. Wahlbeck, <u>ibid.</u>, 49, 1617 (1968).
- 87) J. W. Ward, AEC Report LA-3509, Los Alamos, NM, Jan. 1966.
- 88) J. W. Ward, <u>J. Chem. Phys.</u>, 47, 4030 (1967).
- 89) R. D. Freeman and J. G. Edwards, "Transmission Probabilities and Recoil Force Correction Factors for Conical Orifices" in "The Characterization of High-Temperature Vapors," J. L. Margrave, Ed., John Wiley and Sons, Inc., New York, NY, 1967, Appendix C.
- 90) K. D. Carlson, P. W. Gilles, and R. J. Thorn, <u>J. Chem. Phys.</u>, 38, 2064 (1963).
- 91) E. W. Balson, <u>J. Phys. Chem.</u>, 65, 115 (1961).
- 92) E. Storms, <u>J. Hi. Temp. Sci.</u>, 1, 456 (1969).
- 93) W. Parrish, "Advances in X-ray Diffraction," Centurex Publishing Co., Eindhoven, 1962.
- 94) C. M. Lederer, J. M. Hollander, and I. Perlman, "Table of Isotopes," 6th Ed., John Wiley and Sons, Inc., New York, NY, 1967.
- 95) H. J. Kostkowski and R. D. Lee, "Theory and Methods of Optical Pyrometry," National Bureau of Standards Monograph 41, U. S. Government Printing Office, Washington, DC, 1962.
- 96) J. L. Margrave, "Physiochemical Measurements at High Temperature,"
 J. Bockris, J. White, and J. Mackenzie, Eds., Academic Press, Inc.,
 New York, NY, 1959, Chapter 2.

- 97) P. A. Pilato, Ph. D. Thesis, Michigan State University, East Lansing, MI, 1968.
- 98) G. N. Lewis and M. Randall, "Thermodynamics," Revised by K. S. Pitzer and L. Brewer, McGraw Hill Book Co., Inc., New York, NY, 1961, Chapter 27.
- 99) G. N. Lewis and M. Randall, ibid., Chapter 15 and Appendix 7.
- 100) D. R. Stull and H. Prophet, "The Calculation of Thermodynamic Properties of Materials over Wide Temperature Ranges," in "The Characterization of High-Temperature Vapors," J. L. Margrave, Ed., John Wiley and Sons, Inc., New York, NY, 1967, Chapter 13.
- 101) D. R. Stull and H. Prophet in "JANAF Interim Thermochemical Tables," D. R. Stull, Project Director, Dow Chemical Co., Midland, MI, 1960, pp 3-16.
- 102) E. A. Wood, "Crystal Orientation Manual," Columbia Univ. Press, New York, NY, 1963, p 60.
- 103) N. F. M. Henry and K. Lonsdale, Eds., "International Tables for X-Ray Crystallography," Vol. I, International Union of Crystallography, Kynoch Press, Birmingham, 1952.
- 104) N. F. M. Henry, H. Lipson, and W. A. Wooster, "Interpretation of X-Ray Diffraction Photographs," Macmillan Co., London, 1951.
- 105) T. C. Furnas and D. Harker, Rev. Sci. Instrum., 26, 449 (1955).
- 106) H. Goldstein, "Classical Mechanics," Addison-Wesley Press, Cambridge, MA, 1950, p 107.
- 107) T. Johannson, Naturwissenschaften, 20, 758 (1932).
- 108) U. W. Arndt and B. T. M. Willis, "Single Crystal Diffractometry," Cambridge Univ. Press, Cambridge, 1966, pp 265-267.
- 109) T. C. Furnas, <u>Trans. Am. Cryst. Assoc.</u>, 1, 67 (1965).
- 110) M. J. Buerger, "Crystal Structure Analysis," John Wiley and Sons, Inc., New York, NY, 1960, Chapter 3.
- 111) M. J. Buerger, ibid., Chapter 7.
- 112) U. W. Arndt and B. T. M. Willis, "Single Crystal Diffractometry," Cambridge Univ. Press, Cambridge, 1966, pp 286-288.
- 113) C. H. MacGillavry, G. D. Reick, and K. Lonsdale, Eds., "International Tables for X-Ray Crystallography," Vol. III, International Union of Crystallography, Kynoch Press, Birmingham, 1962.

- 114) M. J. Buerger, "Vector Space," John Wiley and Sons, Inc., New York, NY, 1959.
- 115) H. Lipson and W. Cochran, "The Determination of Crystal Structures," G. Bell and Sons, Ltd., London, 1966.
- 116) D. H. Templeton and C. H. Dauben, <u>J. Amer. Chem. Soc.</u>, 76, 5237 (1954).
- 117) W. R. Busing and H. A. Levy, <u>ORNL-3832</u>, Oak Ridge, TN, Sep. 1965, p 110-150.
- 118) W. R. Busing and H. A. Levy, ORNL-TM-229-4059, Oak Ridge, TN, 1964.
- 119) D. T. Cromer and J. T. Waber, Acta Crystallogr., 18, 104 (1965).
- 120) A. C. Parr and F. A. Elder, <u>J. Chem. Phys.</u>, 49, 2665 (1968).
- 121) L. Brewer, G. R. Somayajulu, and E. Brackett, Chem. Rev., 63, 111 (1963).
- 122) "JANAF Interim Thermochemical Tables," D. R. Stull, Project Director, Dow Chemical Co., Midland, MI, 1960 and Supplements.
- 123) G. N. Lewis and M. Randall, "Thermodynamics," Revised by K. S. Pitzer and L. Brewer, McGraw Hill Book Co., Inc., New York, NY, 1961, p 420.
- 124) E. F. Westrum, Jr., "Advances in Chemistry Series, No. 71, Lanthanide/Actinide Chemistry," R. F. Gould, Ed., American Chemical Society, Washington, D. C., 1967, pp 25-50.
- 125) W. M. Latimer, "Oxidation Potentials," 2nd Edition, Prentice Hall, Englewood Cliffs, NJ, 1952, Appendix III.
- 126) C. E. Wicks and F. E. Block, "Thermodynamic Properties of 65 Elements Their Oxides, Halides, Carbides and Nitrides," U. S. Department of the Interior, Bureau of Mines Bulletin 605, U. S. Government Printing Office, Washington, D. C., 1963.
- 127) R. Hultgren, R. L. Orr, P. D. Anderson, and K. K. Kelley, "Selected Values of Thermodynamic Properties of Metals and Alloys," John Wiley and Sons, Inc., New York, NY, 1963.
- 128) R. C. Feber, AEC Report LA-3164, Los Alamos, NM, 1965.
- 129) R. E. Loehman, R. A. Kent, and J. L. Margrave, <u>J. Chem. Eng.</u>

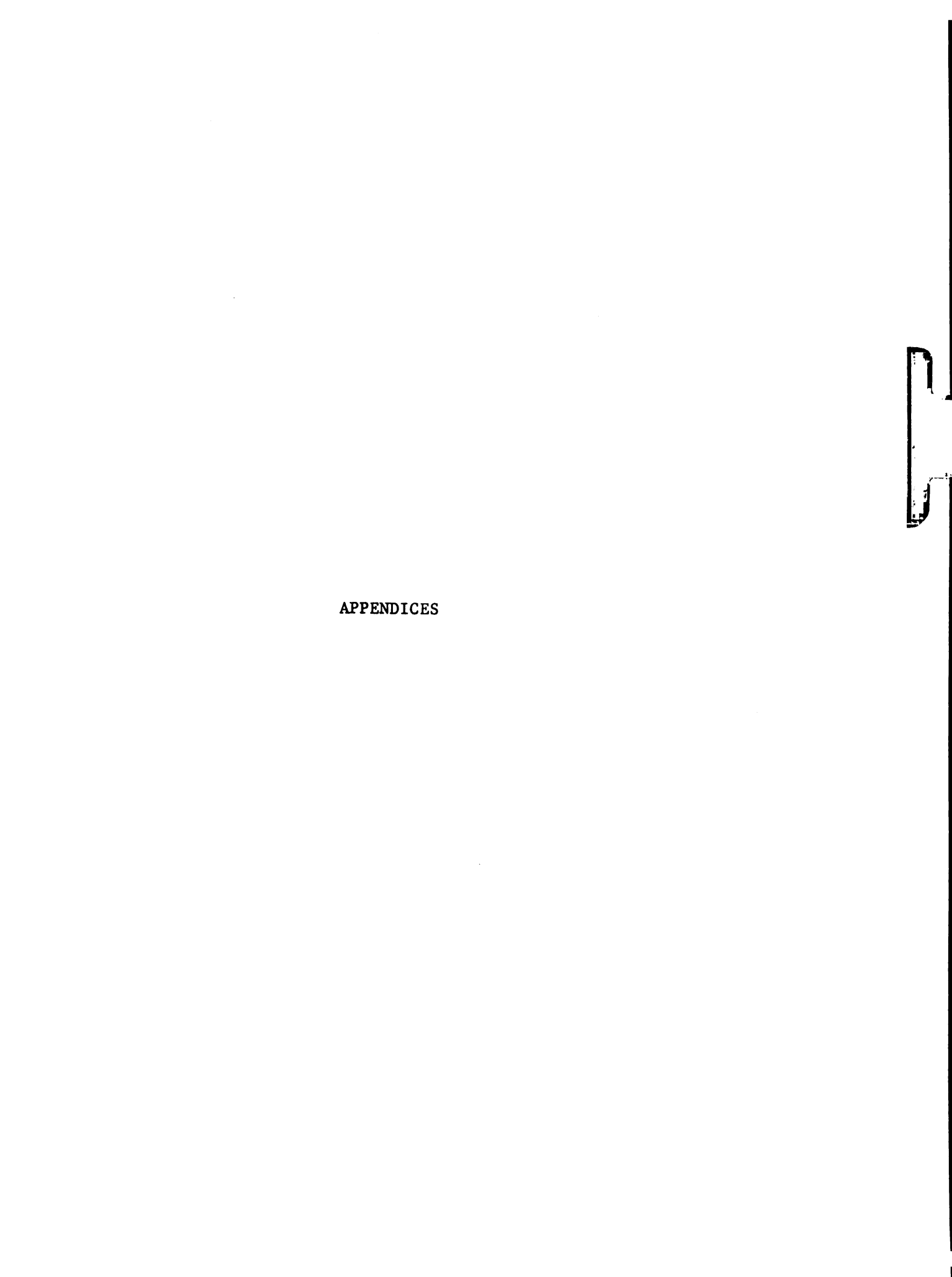
 <u>Data</u>, 10, 296 (1965).
- 130) J. Etienne, <u>Bull. Soc. Fr. Mineral. Cristallogr.</u>, 92, 134 (1969).
- 131) C. Dagron, J. Etienne, J. Flahaut, M. Julien-Pouzol, P. Laruelle, N. Rysanek, N. Savigny, G. Sfez, and F. Thevet in "8th Rare Earth Research Conference," T. A. Henrie and R. E. Lindstrom, Eds., Reno, NV, Apr. 1970, pp 127-139.

- 132) L. Pauling, "The Nature of the Chemical Bond," 3rd Edition, Cornell Univ. Press, Ithaca, NY, 1960.
- 133) A. F. Wells, "Structural Inorganic Chemistry," 3rd Edition, Oxford Univ. Press, Oxford, 1962.
- 134) J. L. Haord and J. D. Grenko, Z. Kristallogr., 87, 110 (1934).
- 135) W. Feitknecht, Fortschr. Chem. Forsch., 2, 670 (1953).
- 136) C. W. Koch, A. Broido, and B. B. Cunningham, <u>J. Amer. Chem.</u>
 <u>Soc.</u>, 74, 2349 (1952).
- 137) C. W. Koch and B. B. Cunningham, <u>ibid.</u>, 75, 796 (1953).
- 138) C. W. Koch and B. B. Cunningham, <u>ibid.</u>, 76, 1471 (1954).
- 139) J. T. Mason and P. Chiotti, <u>Trans. Met. Soc. AIME</u>, 242, 1176 (1968).
- 140) J. D. Corbett, D. L. Pollard, and J. E. Mee, <u>Inorg. Chem.</u>, 5, 761 (1966).
- 141) R. G. Bedford and E. Catalano in "8th Rare Earth Research Conference," T. A. Henrie and R. E. Lindstrom, Eds., Reno, NV, Apr. 1970, pp 213-223.
- 142) B. Prager and P. Jacobsen, Eds., "Beilstein Handbuch der Organischen Chemie," Vol. I, Springer Verlag, Berlin, 1918, p 90.
- 143) J. J. Stezowski, Ph. D. Thesis, Michigan State University, East Lansing, MI, 1968.
- 144) J. D. H. Donnay, Ed., "Crystal Data Determinative Tables," 2nd Edition, American Crystallographic Assn., Washington, D. C., 1963, p 841.
- 145) O. Lindqvist and F. Wengelein, Ark. Kemi, 28, 179 (1967).
- 146) S. Samson and W. W. Schuelke, Rev. Sci. Instrum., 38, 1273 (1967).
- 147) W. L. Bond, Acta Crystallogr., 13, 814 (1960).
- 148) H. J. Neff, Arch. Eisenhuettenw., 34, 903 (1963); Siemens Pamphlet Eg 4/10e, Siemens and Halske Aktiengesellschaft, Karlsruhe, 1964.
- 149) R. A. Kent, Ph. D. Thesis, Michigan State University, East Lansing, MI, 1963.

APPENDIX I: Properties of the Ytterbium Halides.

Compound Color	Color	(D _e) du	(°C) bp(°C)	Symmetry	Type	Lattice Parameters		298°K	
				•		(A)	-∆H g	-∆H °	S
							kcal mole ⁻¹	1e ⁻¹	en
YbF3	white	1157	(2500)	hex/orth	YF3/ LnF3	a=6.99; c=8.32/ a=6.22; b=6.79; c=4.34	(376)	(09)	(56)
YbF2	l	1407	(2650)	cubic	CaF ₂	a=5.57	(280)	(75)	(20)
TbC13	white	865	(dec)	monoclin.	A1C13	a=6.73; b=11.65; c=6.38; B=110.4	229.4	1	(38)
YbC12	green	702	(2242)	orthorh.	CeSI	a=6.69; b=13.15; c=6.94	181.8	61.2	31
YbBr ₃	white	odmooap	nposes	rhomboh.	FeC13	a=6.95; c=19.11	(185)	i	(77)
YbBr ₂	green	613 (2	(2100)	orthorh.	CaBr ₂	a=6.63; b=7.05; c=4.35	(157)	(48)	(36)
Yb13	white	decompo	nposes	hexagonal	Bil3	a=7.43; c=20.72	(143)	1	(41)
Yb12	black	772 (1	(1600)	hexagonal	Cd (0H) 2	a=4.50; c=6.97	(135)	(37)	(40)

Values enclosed in parentheses are estimated.



APPENDIX II: Orientation and Angle Setting Program

This program was written under the title B-101 by J. Gvildys of the Applied Mathematics Division of Argonne National Laboratory. The program is intended for use with goniostats for obtaining accurate three dimensional diffraction data without the necessity of precise alignment of the crystal. The input consists of a limited number of indexed reflections, their measured cradle settings of 2θ , χ , and ϕ , and the wavelength of the radiation employed. Crystal lattice and goniostat constants are computed by the method of least squares from the input data. From the determined constants of the experiment, the program generates for each (hkl) reflection the instrument angles 2θ , χ , and ϕ .

First, least squares constants, (A,B,C,D,E,F), are determined by minimization of the function:

$$\sum_{i} W_{i} \{ (h_{i}A + k_{i}B + \ell_{i}C + 2h_{i}k_{i}D + 2h_{i}\ell_{i}E + 2k_{i}\ell_{i}F) - \frac{4 \sin^{2}\theta_{i}}{\lambda^{2}} \}^{2}$$

where W_{i} is the weight assigned to the i-th reflection. Using the constants determined above, the cell volume is computed by:

$$V = 1/(ABC - AF^2 - BE^2 - CD^2 + 2FED)^{1/2}$$

and the unit cell constants calculated from:

$$a = V(BC - F^2)^{1/2}$$

$$b = V(AC - E^2)^{1/2}$$

$$c = V(AB - D^2)^{1/2}$$

$$\alpha = \cos^{-1}\{(ED - AF)/[(AC - E^2)(AB - D^2)]^{1/2}\}$$

$$\beta = \cos^{-1}\{(DF - BE)/[(AB - D^2)(BC - F^2)]^{1/2}\}$$

$$\gamma = \cos^{-1}\{(FE - CD)/[(BC - F^2)(AC - E^2)]^{1/2}\}.$$

Second, the components of a unit vector $\underline{\mathbf{A}}(\mathbf{u}\mathbf{v}\mathbf{w})$ which lies along the ϕ -axis of the goniostat when χ = 0 are determined by minimization of the function:

$$\sum_{i} \cos^{2} \chi_{i} \left(h_{i} u + k_{i} v + \ell_{i} w - \frac{\sin \chi_{i}}{d_{i}} \right)$$

then:

$$\chi_i^{\text{calc}} = \sin^{-1} \left[d_i(h_i u + k_i v + \ell_i w) \right].$$

Third, the components of a unit vector $\underline{B}(xyz)$ which is perpendicular to \underline{A} and lies in the χ -plane of the instrument when ϕ = 0 are determined by minimization of the function:

$$\sum_{i} \{\cos \chi_{i}^{\text{calc}} d_{i}[(h_{i}A + k_{i}D + \ell_{i}E)x + (h_{i}D + k_{i}B + \ell_{i}F)y + (h_{i}E + k_{i}F + \ell_{i}C)z] - \cos \chi_{i}^{\text{calc}} \cos \phi\}^{2}$$

then:

$$\phi_{\mathbf{1}}^{\text{calc}} = \tan^{-1} \left(\underbrace{v_{\mathbf{h}_{\mathbf{1}}\mathbf{U}}^{\mathbf{h}_{\mathbf{1}}\mathbf{U}} + k_{\mathbf{1}}\mathbf{V} + \ell_{\mathbf{1}}\mathbf{W}}_{\mathbf{h}_{\mathbf{1}}\mathbf{X}} \right),$$

where

$$U = y[u(DF - BE) + v(ED - AF) + w(AB - D^{2})]$$

$$- z[u(FE - CD) + v(AC - E^{2}) + w(ED - AF)]$$

$$V = z[u(BC - F^{2}) + v(FE - CD) + w(DF - BE)]$$

$$- x[u(DF - BE) + v(ED - AF) + w(AB - D^{2})]$$

$$W = x[u(FE - CD) + v(AC - E^{2}) + w(ED - AF)]$$

$$- y[u(BC - F^{2}) + v(FE - CD) + w(DF - BE)]$$

$$X = xA + yD + zE$$

$$Y = xD + yB + zF$$

$$Z = xE + vF + zC.$$

The angles $(2\theta, \chi, \phi)$ are then calculated for each (hkl) reflection permitted under the various extinction, octant, and angle options selected by the user.

APPENDIX IIIA: Ytterbium Trichloride Hexahydrate

		rved		lated
hkl	Relative Intensity	d-value (Å)	Relative Intensity	d-value (Å)
010	30*	6.484	20	6.524
10 I	80	6.252	51	6.288
101	90	5.871	59	5.854
110	20	5.369	24	5.393
011	20	4.988	26	5.010
200	60	4.776	46	4.792
111	20	4.494	23	4.527
111	20	4.342	28	4.357
002	100	3.904	100	3.910
210	10	3.846	7	3.862
211	10	3.521	7	3.546
211	10	3.376	7	3.384
012	20	3.353	14	3.354
202	20	3.128	16	3.144
21	10	3.014	1	3.011
202	20	2.932	20	2.927
10	30	2.859	27	2.869
12	10	2.832	3	2.832
11	20	2.644	14	2.638
Ε0	30	2.564	15	2.563
21	50	2.509	39	2.517

^{*}Visually estimated.

101
APPENDIX IIIB: Intermediate Ytterbium Chloride (YbCl_{2.26})

Relative Intensity	d-value (Å)	Relati ve Intensity	d-value (Å)
7	9.24	4	4.24
1	6.46	1	3.96
4	5.97	10	3.88
3	5.76	1	3.48
1	5.32	2	3.41
3	4.77	4	3.38
2	4.39	2	3.36

APPENDIX IIIC: Ytterbium Dichloride

hkl	Relative Intensity	d-value (Å)	hkl	Relative Intensity	d-value (Å)
020	2	6.575	122	2	2.786
021	4	4.768	221	3	2.739
111	2	4.520	141	1	2.715
121	10	3.884	230	2	2.660
002	5	3.462	202	7	2.406
200	4	3.347	042	8	2.384
040	4	3.288	240	8	2.345
210/13	1 1	3.243	142	6	2.246
102	1	3.075	023	4	2.178
022	1	3.064	311	2	2.096
112	2	2.995	123	5	2.071
041	1	2.970	321	7	2.021

		1

APPENDIX IIID: Ytterbium Oxidechloride

hkl*	Relative Intensity	d-value (Å)	hkl*	Relative Intensity	d-value (Å)
003	9	9.438	110	10	1.863
006	5	4.668	114	7	1.827
101	7	3.215	116	5	1.729
102	8	3.153	201	5	1.611
009	6	3.100	202	4	1.604
104	7	2.939	119	6	1.596
105	7	2.798	204	5	1.571
107	4	2.510	205	4	1.550
108	3	2.369	207	3	1.495
00.12	4	2.321	208	2	1.467
10.10	2	2.105	11.12	6	1.453
10.11	2	1.990	20.10	2	1.392

^{*}Indexing based on a=3.726, c=27.80 Å

APPENDIX IIIE: Triytterbium Tetraoxidechloride Preparation

Relative Intensity	d-value (Å)	Relative Intensity	d-value (Å)
10	9.339*	6	2.996
3	4.804	7	2.594
2	4.244	1	2.031
3	3.660	8	1.850
4	3.186*	5	1.883*
5	3.086*	5	1.814

^{*}Possible coincidence with YbOCl

APPENDIX IV: Equilibrium Pressure and Third-Law Enthalpy Data

$\frac{10^4}{T}$ (°K ⁻¹)	-log P (atm)	$^{\Delta ext{H}^{\circ}_{\mathbf{V}}}$ 298 (kcal mole-1)
7.49	4.38	58.25
8.53	5.70	60.74
7.96	4.97	58.47
7.73	4.66	59.84
7.36	4.21	60.06
7.76	4.73	59.20
7.98	4.94	58.35
8.18	5.20	60.74
8.18	5.26	59.06
8.26	5.32	59.40
8.33	5.38	60.72
8.77	5.54	59.83
8.57	5.72	60.61
9.55	7.00	59 .69
9.41	6.78	60.38
9.18	6.50	60.47
9.18	6.50	60.42
8.98	6.24	61.19
8.52	5.64	60.12
8.32	5.38	58.70
8.76	5.93	60.60
9.02	6.35	60.95
9.10	6.36	60.95

APPENDIX IV: (cont.)

8.58	5.76	60.64
8.28	5.37	58.63
8.26	5.31	60.63
8.02	5.01	61.02
8.64	5.82	59.77
7.87	4.72	59.60
7.80	4.72	59.60
7.70	4.60	59 .79
7.60	4.54	60.36
7.47	4.37	60.14
7.91	4.88	59.11
6.74	3.70	60.89
7.12	3.97	59.23
7.22	3.99	59.96
7.28	4.09	60.31
7.32	4.14	58.88
7.56	4.36	59.56
7.84	4.70	60.04
7.83	4.61	60.16
7.33	4.20	59.52
7.60	4.46	59.87
7.65	4.58	59.52
8.06	5.02	59.15
8.40	5.51	59.83
8.60	5.79	58.95
8.47	5.63	59.74

APPENDIX V: Thermodynamic Values for Data Reduction.

105

Phase	-∆H _f 298	S 2 98	-(G _T -H ₂₉₈)/T (eu)			
	(kcal mole ⁻¹)	(eu)	500	1000	150 0 'K)	2000
Yb ₂ 0 ₃ (s)	433.68 ¹²⁴	31.8 ¹²⁴				
Yb(s)	0.0	13.1124		17.8	21.3	
Yb(g)	-36.35 ¹²⁷					47.412
YbCl ₂ (s)			30 ³⁰	40	48	57
YbC1 ₂ (g)			72	78	82	86
H ₂ (g)	0.0			35		
H ₂ O(g)	60		41	47	51	53
C1(g)	29		40	42	44	45